Unmanned Solar Powered Airship Concept Evaluation

Critical Design Report

Document Reference No.: USPACE-CDR-A2

Document Status: RELEASED

Authors

Dries Agten
Ishan Basyal
Bastian Hacker
Morten Olsen
Jan Sommer
Tiago Rebelo
Mauro Aja Prado
Pedro Cervantes
Zhou Hao
Oliver Porges
Anuraj Rajendraprakash
Omair Sarwar

Supervisors

Kjell Lundin
Thomas Kuhn

Project Manager

Morten Olsen

November 22, 2012
Luleå University of Technology
Rymdcampus, Kiruna, Sweden

Normative References

Table 1 – *Normative References for this document*

Document title	Doc. Ref. No.	Doc. status
Preliminary Design Report	USPACE-PDR-A1	Review

Document Change Record

Table 2 – *Document Change Record for this document*

Doc. version	Change date	Change Description
USPACE-CDR-A1	11 Sep. 2012	1st release
USPACE-CDR-A2	22 Nov. 2012	Implemented review comments from supervisors, added new student and supervisor, added comment on extended course credits for some students, added EPS thermal calculations and updated EPS block diagram and telemetry/telecommand table.

Acronyms

ADS Attitude Determination System

BCR Battery Charge Regulator

BJT Bipolar Junction Transistor

CC Constant Current

CDR Critical Design Review

CM Current Mode

COTS Commercial Off-The-Shelf

CPU Central Processing Unit

DCM Discontinuous Conduction Mode

DM Development Model

DSP Digital Signal Processor

ECSS European Cooperation for Space Standardization

EGSE Electrical Ground Support Equipment

EKF Extended Kalman Filter

EMC Electromagnetic Compatibility

EMI Electromagnetic Interference

EPS Electrical Power System

ESC Electronic Speed Control

ESR Equivalent Series Resistor

FM Flight Model

FRR Flight Readiness Review

GPS Global Positioning System

I^2C Inter-Integrated Circuit

IC Integrated Circuit

IRF Swedish Institute of Space Physics

ITPU Imaging and Tracking Payload Unit

ITU International Telecommunication Union

LDO Low-dropout

LiPo Lithium-Polymer

LTU Luleå University of Technology

MCC Motor Control and Communication

MCU Micro-Controller Unit

MEA Main Error Amplifier

MGSE Mechanical Ground Support Equipment

MOSFET Metal-Oxide-Semiconductor Field-Effect Transistor

MPP Maximum Power Point

MPPT Maximum Power Point Tracking

MPPTU Maximum Power Point Tracking Unit

MSE Mechanical Structure and Envelope

NTC Negative Temperature Coefficient

OpAmp Operational Amplifier

PCB Printed Circuit Board

PDR Preliminary Design Review

PSA Pressure Sensitive Adhesive

PTC Positive Temperature Coefficient

PWM Pulse Width Modulation

RHPZ Right Half Plane Zero

SAR Solar Array Regulator

SD Secure Digital

SMD Surface-Mount Device

SoC System on Chip

SPA Solar Powered Airship

SSC Swedish Space Corporation

TBD To Be Decided

U-SPACE Unmanned Solar Powered Airship Concept Evaluation

UART Universal Asynchronous Receiver/Transmitter

UAS Unmanned Aircraft System

UAV Unmanned Aerial Vehicle

USB Universal Serial Bus

UVLO Under-Voltage Lock-Out

List of Figures

List of Tables

Contents

Chapter 1

Introduction

Unmanned Solar Powered Airship Concept Evaluation (U-SPACE) is a student project at the Rymdcampus of the Luleå University of Technology (LTU) in Kiruna under the supervision of Kjell Lundin (Swedish Institute of Space Physics (IRF)) and Alf Wikström (LTU). It is supported by IRF and LTU. The goal of this project is to prove the concept of a small-scale student-built unmanned Solar Powered Airship (SPA). The solar cells that power the airship are mounted on a gas-filled envelope, with forward propulsion being achieved by propellers mounted onto the same envelope. The airship communicates via two separate wireless connections with a controller and a ground station. These communication channels enable human control over the airship, together with the retrieval of housekeeping and scientific payload data. The payload data consists of measurements from several sensors (magnetometer, accelerometer, gyroscope and Global Positioning System (GPS)) and images collected by a small on-board camera. On the ground station, the image data and the sensor data are combined to construct an aerial map of the flight environment.

The concept of a SPA has attracted major interest in recent years [1, 2, 3, 4, 5, 6, 7, 8, 9]. Applications for this type of airship reach far and wide, ranging from passenger and cargo transport [2, 5, 7, 8, 9] over scientific research [3] and surveillance [1, 6, 7] to planetary exploration [4]. In Scandinavia there have been several studies on using airships for the transport of windmill structures [9, 10] and the windmill company Vestas has filed a patent on this method [11]. The actual implementation of the SPA concept varies greatly. Solar Ship [8] is a hybrid of an aircraft and an airship, while Project Sol'r [5] has the intention of building a manned SPA, in contrast to many of the other implementations. Some airships are intended for low-altitude flight [5, 7], while other airships are meant to fly at 18 km altitude or above [1, 3, 6]. Regardless of their exact implementation or application all SPAs benefit greatly from the advantages of this concept: simple flight control, reduced fossil fuel consumption and access to long duration flights. Apart from these inherent strong points, other advantages of SPAs are the possibility for autonomous take-off and landing, the elimination of large infrastructures like airports, reduced weather constraints and relatively low costs [1, 2].

Even though many research groups and commercial companies have investigated the possibilities of SPAs, very few student-driven projects exist. Projet Sol'r [5] for example, created by a team of French students, has the intention of piloting a SPA across the English Channel. This team is the exception in all projects discussed previously. The above-mentioned advantages of SPAs and the fact that few student projects exist, were the main drivers for the creation of the U-SPACE project at LTU.

1.1 Hardware

The hardware for the U-SPACE project can be divided into four subsystems, as visualized in the block diagram of Figure 1.1. This hardware includes both the airborne parts (the SPA) and the ground-based parts (ground station and controller).

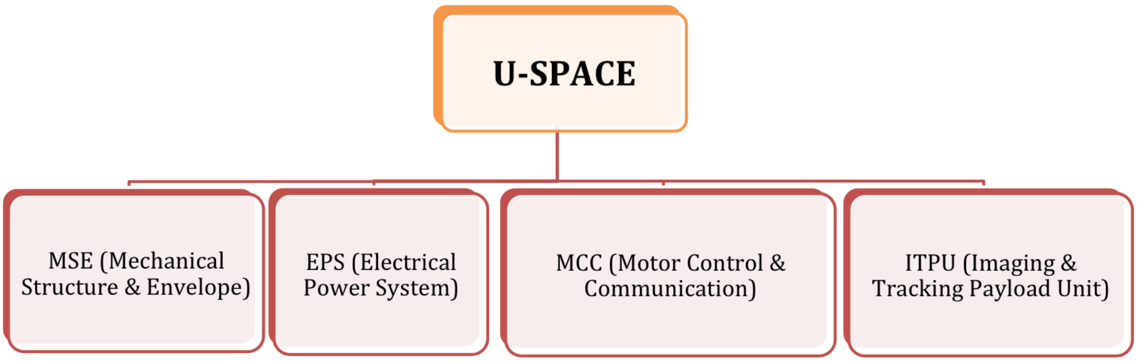

Figure 1.1 – *Hardware block diagram of the U-SPACE project*

1.1.1 On-board Hardware

The first subsystem is the Mechanical Structure and Envelope (MSE). This subsystem is the principal mechanical structure of the airship. It includes a gas-filled envelope, a payload bay and structures to mount both the solar cells and the propellers. This subsystem is the support for all other subsystems and provides the lift to allow the SPA to fly. More information can be found in chapter 3. The second subsystem, the Electrical Power System (EPS), is responsible for generating solar power, distributing this power to all other subsystems and storing the generated energy when required. It makes use of the MSE subsystem which supports the solar cells, while it also allows both forward propulsion and the generation of scientific payload data. Chapter 4 provides the details on this subsystem. The third subsystem, Motor Control and Communication (MCC), takes care of the forward propulsion of the airship by employing propellers mounted onto motors. The structural link to the airship is the responsibility of the MSE, while power is provided by the EPS. The motors are controlled via a wireless connection, which is also the responsibility of this subsystem. A more thorough discussion can be found in chapter 5. The final subsystem, the Imaging and Tracking Payload Unit (ITPU), is the scientific payload of the SPA. It consists of several different sensors (including a magnetometer, an accelerometer, a gyroscope and a GPS) mounted inside the payload bay (part of the MSE). The data from these sensors is processed with the help of a Micro-Controller Unit (MCU). The payload bay also contains a camera which can take pictures from the ground that are saved on board or transmitted to a ground station via a second wireless connection. The sensor data is also sent to the ground station via this wireless connection. The power for the sensors, the MCU, the camera and the wireless connection is provided by the EPS. Chapter 6 discusses this subsystem in more detail.

1.1.2 Ground-based Hardware

The hardware for the ground station and for the wireless control are respectively part of the ITPU and MCC subsystems (see chapters 6 and 5 respectively). This hardware consists of a receiver for the scientific payload data and a transmitter/receiver for the control of the SPA. In order to present the scientific payload data from the sensors and the camera, a means to visualize this ITPU data is required as well.

1.2 Software

The software required for the U-SPACE project is only present in the on-board ITPU subsystem and in the ground station used to receive the scientific payload data from this subsystem. The other subsystems do not require the development of any software.

1.2.1 On-board Software

The software on board the SPA reads the data from the sensors (magnetometer, accelerometer, gyroscope and GPS) and fuses these data in order to obtain more accurate information about the orientation and position of the airship. The software is also responsible for sending this scientific payload data to the ground station via the dedicated wireless connection. Finally the on-board software is needed to control the camera and to take pictures from the ground below the airship. The pictures are saved on board or sent to the ground station via a wireless connection. A description of this software can be found in chapter 6.

1.2.2 Ground-based Software

The ground station also requires the development of some software. This software is mainly responsible for receiving sensor data from the airship via the wireless connection, but it is also needed for the visualization of this data. It runs an algorithm that combines the data from the sensors and the images taken by the camera in order to obtain a complete aerial map of the landscape over which the SPA is flying. Once again chapter 6 provides more details.

1.2.3 Operational Modes

With the development of the on-board and ground-based software modules, several operational modes related to the scientific payload become possible in the U-SPACE project. The basic modes are listed below:

1. Read out data from sensors and data fusion
2. Control the camera to take pictures from the ground
3. Combination of mode 1 and mode 2

Chapter 2

Goals and Constraints

2.1 Project Goals

The principal goal of the U-SPACE project is to bridge the gap between a student-driven engineering project and the concept of an unmanned SPA. As very few examples of this type of design exist [5], much is to be gained from the project. The goal of this project is thus designing, building and testing a small-scale SPA for low altitude flight, including support for a scientific payload. The basic targets are listed below:

1. Design of a small unmanned SPA capable of forward propulsion and steering, powered by solar cells and including a scientific payload

2. Flight test of this SPA at low altitude

Initially, it was also considered to build our own envelope. However, due to time constraints and an arising opportunity to borrow a blimp from Esrange, this became our choice of envelope.

2.2 Project Constraints

The design, construction and test of a small unmanned SPA is susceptible to many constraints, all of which have to be identified, examined and finally dealt with. These constraints take many forms, but may be divided into four categories: functionality, resources, environment and law.

2.2.1 Functionality

The U-SPACE project, being a proof of concept, consists of designing, building and testing a small version of a SPA with a limited scientific payload. Therefore reasonable limits have to be taken into account for some technical parameters. These parameters and their limits are listed below in Table 2.1.

Table 2.1 – *Functional parameters and limits*

Parameter	Lower limit	Upper limit
Total mass	-	$4.5\,kg$
Flight altitude	$2\,m$	$100\,m$
Electrical power	-	$40\,W$
Forward velocity	-	$1\,m/s$

2.2.2 Resources

Since the U-SPACE project is a student project supported by LTU and IRF, the available resources are limited. This imposes stringent constraints on all phases of the project. The cost of this student project is limited by its approved budget, an initial sum of 14,000 SEK is provided by LTU(2000 SEK per European student). More funding can be applied for if required, but the budget nevertheless remains limited. This constraint implies a careful selection of components and the use of innovative engineering solutions throughout the entire project.

The time available for this project is also constrained, being a student project that has to be realized in concurrence with other academic duties. The estimated time frame is therefore between 2 and 6 months for a first prototype capable of test flight.

The final resource is related to the previously mentioned functionality. With a limited number of team members that have limited expertise in the field of airships, the project has to be technically balanced, taking into account the capabilities of the members of the team (see chapter 12).

2.2.3 Environment

The SPA that is developed during the U-SPACE project has to be tested outdoors in a final stage. Since the U-SPACE project is being executed in the city of Kiruna during the spring, summer and early autumn, it is important to take the environmental conditions during this period of the year into account. The most important conditions between the months May and September are listed in Table 2.2 [12].

Table 2.2 – *Environmental conditions*

Parameter	Lower boundary	Upper boundary	Remarks
Temperature	$-7° \, C$	$22° \, C$	Worst-case $10 - 90$ percentile bands
Wind speed	$1 \; (3) \, m/s$	$6 \; (9) \, m/s$	Daily averages (worst-case $10 - 90$ percentile bands)
Probability of precipitation	61%	63%	Daily average. Mostly light rain/snow to moderate rain/snow
Cloud cover	83%	85%	Median cloud cover (mostly cloudy)
Solar incidence angle	46°	57°	See section 4.2.3

2.2.4 Law

The final constraints that have to be taken into account are possible legal issues that may arise during the construction and testing phase of the SPA. A first legal constraint is the compliance to the International Telecommunication Union (ITU) Radio Regulations [13] when using wireless connections. Secondly, when flying the SPA, the Swedish Transport Agency's regulations on Unmanned Aircraft System (UAS) [14] might have to be taken into account. As the application of these regulations depends on the final mass and size of the prototype airship, this constraint can only be investigated when a prototype is constructed.

2.3 Expected Functionality

Based on the project goals set forth in section 2.1 and taking into account the constraints discussed in the previous section, a realistic prediction of the functionality of the final product of the U-SPACE project can be made. The expected functionality of the small-scale SPA is summarized in Table 2.3.

Table 2.3 – *Expected functionality*

Parameter	Value	Remarks
Autonomy	$2 \, h$	At peak power
Flight altitude	$2 - 20 \, m$[1]	-
Forward velocity	$0.5 - 1 \, m/s$	-
Flight conditions	Daytime	Sunny and calm weather

The other functional constraints presented in section 2.2 will be discussed in subsequent chapters. In the future, when the first prototype gives satisfactory results, this functionality might also be expanded with features like autonomous attitude control and altitude control during flight.

2.4 Fault Tolerance Design and Safety Concept

Since the goal of the U-SPACE project is to design, build and test a prototype of a small-scale SPA, the focus of this project is not on a fault-tolerant SPA design, but rather on performance of the design that meets the project goals. Nevertheless some safety features are included in the design, construction and flight test of the airship. These features will be discussed in the chapters dedicated to the different subsystems and in chapter 11.

2.5 Materials

With the limited time and funding inherent to this student-driven project great care needs to be taken with regards to the selection and processing of the materials. The materials need to be as performant as possible for their specific function while at the same time their cost should be as low as possible. In general all materials should also be as light as possible. The specific material requirements for each subsystem are discussed in subsequent chapters.

With regards to the processing of the materials, low cost is again the main discriminator to select an appropriate technique. Therefore the simplest techniques are preferred during the construction of the airship, with as less mechanical work as possible. A certain amount of experience with such techniques is present in the team, allowing short construction times and limited delays.

Chapter 3

Mechanical Structure and Envelope

The first subsystem is the MSE. It is considered to be the foundation of the entire airship, seeing the fact that it acts as the basis which withstands all external influences and holds all the other subsystems together. This subsystem also includes the device that will be generating the lift for the entire SPA. The fact that now an Esrange blimp is used, rather than a custom-made blimp (due to time constraints), has modified virtually every requirement that was defined in the preliminary design [15]. This chapter will cover the updated requirements and constraints together with a view on the possible alternatives to overcome the problems that are currently being faced. Also the updated design and the construction phase will be presented.

3.1 Functional and Technical Specifications

This section will cover the updated requirements that are the consequences of the choices taken during the course of the project. The functional requirements have of course not changed, but the same cannot be said about the technical requirements.

3.1.1 Functional Requirements

The MSE should have the following properties or be capable of the following functions.

- Aerodynamic stability
- Support the solar cells, the propulsion system and the scientific payload
- Sufficient lift to overcome the weight of the entire system
- Low diffusivity for the balloon material

3.1.2 Technical Specifications

The previously calculated/estimated parameters have been modified to fit the constraints imposed by the new Esrange blimp. They are presented in Table 6.1.

Table 3.1 – *Technical specifications of Esrange blimp*

Parameter	Value
Length	$4.94\,m$
Diameter	$1.89\,m$
Volume	$15\,m^3$
Maximum lift mass	$2.59\,kg$

Comparing the new available maximum lift mass provided by the blimp, it can be seen that the new total mass is half that of which was initially assumed during the Preliminary Design Review (PDR). This entails that the mass budgets available for each of the subsystems have to be redistributed. For the MSE subsystem in particular, the consequence is a complete redesign of the entire structure, dismissing the initial idea of a rigid structure. The next section explains how the design was modified, also presenting suggestions for the corresponding new structural components.

3.2 Critical Design

As was mentioned in the PDR, the initial mechanical design of the U-SPACE project included the development of a blimp (envelope) that accommodates the solar panels of the EPS, the cargo bay for the ITPU subsystem and the propelling system of the MCC subsystem. An initial sketch of this concept is presented in Figure 3.1.

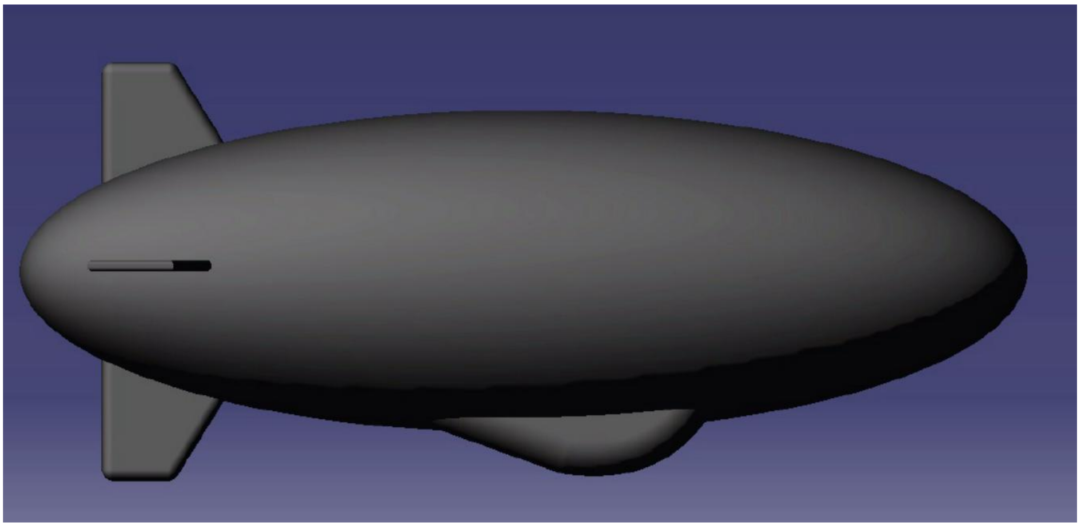

Figure 3.1 – *Initial 3D sketch of the SPA concept*

This simplified view of the mechanical design shows that it included the development of an envelope for the airship. The idea was to attach the solar panels on the top, mounted onto a wired mesh, with the cargo bay located at the bottom together with the propelling system.

However, due to new developments in the project that included the introduction of an already built blimp (envelope), the focus of the mechanical design was changed. The blimp to be used is the *TIF-250* [16], shown in Figure 3.2. This blimp has the capacity to lift a payload of about 2.5 kg, has a length of approximately 5 m and has a diameter (in the center) of about 1.9 m (see Table 6.1).

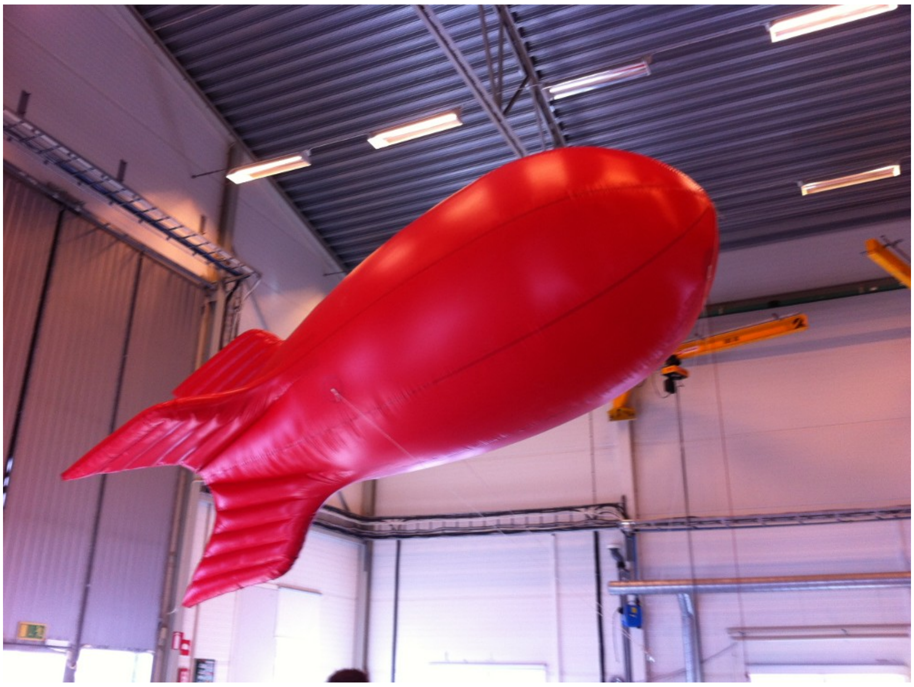

Figure 3.2 – *Test of TIF-250 blimp from Esrange*

This blimp serves the purpose of the U-SPACE project very well, as using it would allow to focus only on the construction of the support for the EPS, on the cargo bay for the payload and on the integration of the propelling system. However, because it is a ready-built blimp with a purpose different than the one envisioned, it is not as lightweight as required. Nevertheless, light structures will be included in the integration of all other systems to remedy this problem.

3.2.1 Envelope

As was mentioned above, the blimp to be used is already built. This blimp is normally used to accurately measure the wind direction. Nevertheless it will have to fit the purpose of the U-SPACE project, due to the lack of time to build a new envelope. The blimp itself thus functions as the envelope.

3.2.2 Cargo Bay

The cargo bay accommodates both the payload and the electronics required for U-SPACE. The main challenge in the construction of this cargo bay is the mass. It has to be lightweight (the maximum total mass of all structures should be less than 1 kg) but at the same time rigid enough to resist some stress during the normal operation of the airship. To achieve this functionality, balsa wood reinforced with carbon fibres is used. Thermal cover film will be wrapped around the cargo bay. The current construction status is shown in Figure 3.3.

Figure 3.3 – *Current construction of the cargo bay*

3.2.3 Power System

The biggest challenge in this project is the accommodation of the power system, taking into account the maximum lift mass and the power requirements that consequently influence the solar panel quantity and mass. The idea is to use a lightweight wired mesh that serves as a support for the solar panels, which are attached to the wires with carbon fibre. This mesh is connected to the blimp by making use of three bands that will go around the blimp, distributing the weight along the envelope. These bands are made of fibre glass reinforced rubber tape. An idea of how the final design could look like is presented in Figure 3.4.

3.2.4 Propelling System

The propelling system is attached to a carbon fibre rod mounted onto the top of the cargo bay. The two motors are attached at the ends of the rod, away from the influence of the envelope and free to achieve their maximum aerodynamic capabilities. A hand sketch of

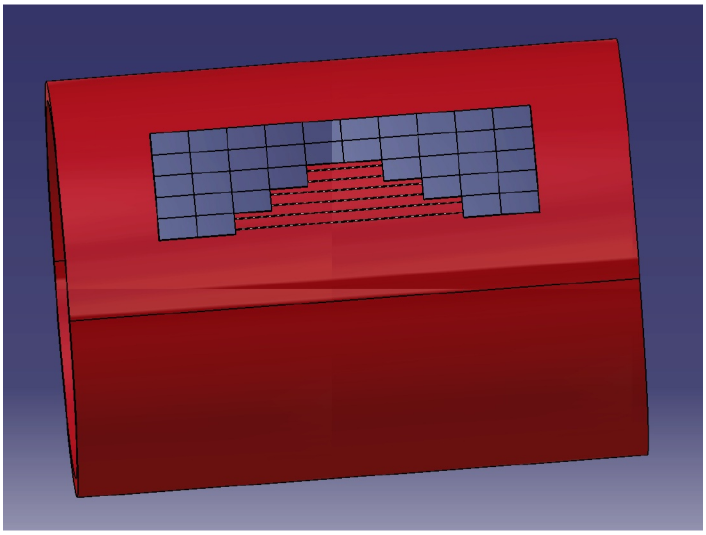

Figure 3.4 – *3D sketch of the integration of the power system*

this principle is shown in Figure 3.5.

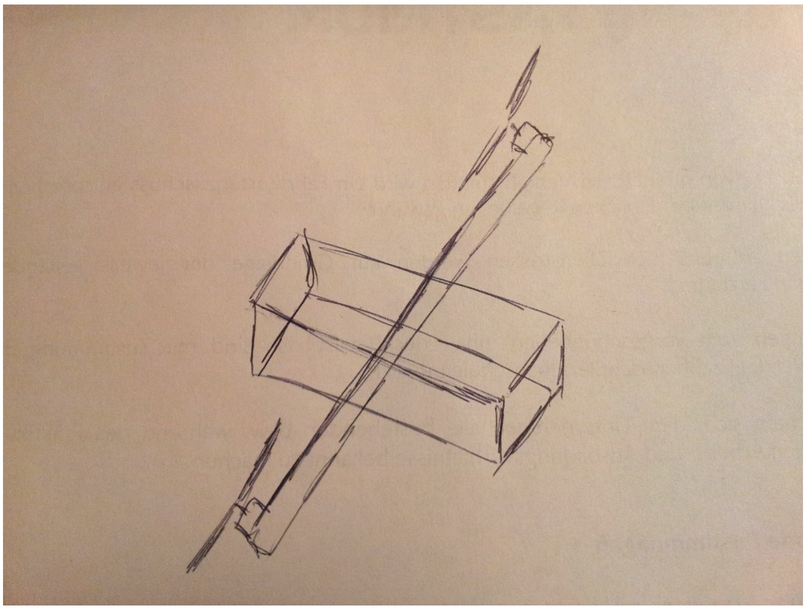

Figure 3.5 – *Hand sketch of the integration of the propelling system*

3.2.5 Mass Budget

A detailed mass budget of the U-SPACE subsystems and their components are listed in Table 3.2.

Table 3.2 – *U-SPACE mass budget*

Subsystem	**Part**	**Weight**	**Budget**
EPS	Solar cells	$590 - 760\,g$[a]	
-	Battery	$122\,g$	
-	Regulators + PCB	$55\,g$	
-	Wiring	?	
-	Mounting	$\sim 15\,g$	
total:		$952\,g$	$1000\,g$
MCC	Motors + Propellers	$68\,g$	
-	ESCs + Receivers	$21\,g$	
-	Wiring	$5\,g$	
-	Xbee-Pro radio	$9\,g$	
-	Motor attachments	$\sim 20\,g$	
total:		$123\,g$	$250\,g$
ITPU	BeagleBoard	$43\,g$	
-	Sensors	$4\,g$	
-	PCB + Wiring	$30\,g$	
-	Etag	$39\,g$	
-	PCB Mounting	$\sim 20\,g$	
total:		$136\,g$	$250\,g$
MSE	Cargo Bay	$60\,g$	
-	Carbon rod	$191\,g$	
-	Envelope mesh	?	-
-	Thermal insulation	$\sim 100\,g$	
total:		$351\,g$	$1000\,g$
system total:		$1.551\,g$	$2,500\,g$

[a]Depends on if solar cell with our without PSA is used

3.3 Future Developments

Only after a careful construction of the different structures that accommodate the required subsystems will it be possible to check if the requirement of the maximum lift mass (the most important requirement of this subsystem) is achieved. The 3D designs, the envisioned materials and previous experience in the field give hope that this constraint will be dealt with. The next steps are to finish the construction of the cargo bay, accommodate the propelling system and then to proceed with the construction of the wiring mesh and the attachment of the solar panels.

3.4 Mechanical Interfaces

The MSE external mechanical interfaces and their planned implementations are listed in Table 3.3.

Table 3.3 – *Mechanical Structure and Envelope external interfaces*

External interface	Implementation
Motors to carbon fiber rod	Attached on small aluminium plates that are fastened to carbon fiber rod using plastic clamps.
Solar cells to envelope mesh	?
Cargo bay to envelope mesh	?
Envelope mesh to blimp	?
ITPU and EPS regulators to cargo bay	Attached with plastic spacers[1] which are glued to cargo bay bottom plate.
Etag to cargo bay	Attached using the battery-housing to battery-sized piece which is glued to cargo bay bottom plate.
Battery and MCC receiver to cargo bay	Attached with Velcro glued to cargo bay bottom plate.

3.4.1 Accommodation Requirements

One of the main criteria for all mechanical assemblies is to minimize their weight. Thus low-weight materials like plastic, aluminium and carbon fiber are preferred. Secondly, all assemblies should be easily detachable for part replacement, changes in in mechanical layout, dissembling of subsystems for testing etc.

Chapter 4

Electrical Power System

4.1 Introduction

The EPS provides power to the motors, the on-board computer, the communication system and the payloads. Power is mainly supplied from solar cells but can also be supplied from a battery, when solar power is not available or insufficient.

4.1.1 Changes from PDR to CDR

Table 4.1 lists major design changes from the EPS PDR report.

Table 4.1 – *Design changes from PDR to CDR*

Area of change	Change	Argumentation for change
Total power budget	Increased to $> 40\,W$	Airship total mass and size are increased thus requiring much more power for the motors.
Solar cells	New part	Old solar cell was much heavier than listed in manufacturer datasheet due to a glass cover.
Total system cost	Increased to $> 12000\,SEK$	Increased power and new light-weight solar cells are more expensive.
Solar cell mounting	New part	New solar cell is flexible instead of rigid and can be mounted with Pressure Sensitive Adhesive (PSA).
Battery	New part	A battery that supports much higher discharge currents has been selected which simplifies current limiting circuitry and improves battery efficiency.

4.2 Functional and Technical Requirements

This section describes the functional and technical EPS requirements along with the expected EPS performance.

4.2.1 Functional Requirements

The primary functional EPS requirements are:

- Provide adequate power to motors, other subsystems and payloads
- Prove that flying on solar energy is possible i.e more power produced than consumed

Additional desired requirements are:

- Scalable and flexible system architecture allowing the EPS to be upgraded to higher power levels or re-used in different applications (rover, Unmanned Aerial Vehicle (UAV) etc.)
- Robust design allowing flight in more extreme conditions (altitude, weather etc.)
- Provide adequate protection circuits for battery and loads to prevent any major failure and damage to other subsystem components.
- Optimal design and high performance to increase power capability and minimize system mass

4.2.2 Power Budget and Technical Requirements

The EPS power budget is listed in Table 4.2 and the technical requirements are listed in Table 4.3.

Table 4.2 – *Power budget*

Part/subsystem	**Peak load**	**Average load**
2 x MCC motors	$120\,W$	$\sim 40\,W$
MCC ETag	$100\,mW$	$100\,mW$
MCC Xbee-Pro radio	$10\,mW$	$10\,mW$
ITPU BeagleBoard + sensors	$3\,W?$	$3\,W?$
Total:	$123.11\,W$	$43.11\,W$

Table 4.3 – *Technical requirements for EPS*

Description	**Symbol**	**Value**
Minimum power output	$P_{out,min}$	$40\,W^a$
Maximum mass	$W_{EPS,max}$	$1000\,g$ including solar array
Maximum cost	-	$4000\,SEK^b$
Output voltages	$V_{mainbus}$, V_{5V}	$6.0 - 9.5\,V$ un-regulated and $5\,V$ regulated
Operational temperature	T_{min}, T_{max}	$-20°C\ to\ +45°C$
Battery capacity	C_{bat}	$> 5\,Wh$

[a]Average Solar Array Regulator (SAR) output power including losses
[b]Initial budget for 2 students

4.2.3 Mission and Environmental Constraints

This section discusses the system challenges imposed by the operation environment.

Solar Array Temperature

As was discussed in [15], the optimal operating voltage of the solar cells change with temperature. The EPS must be able to generate optimal power from the solar cells in the full expected temperature range of the environment. This can be achieved using a Maximum Power Point Tracking Unit (MPPTU) which will be discussed in section 4.3.3

Solar Incidence Angle

The flight location of U-SPACE is near Kiruna in Sweden. Figure 4.1 shows the average solar incidence angles in Kiruna for the months June and September [17], considering a flat solar panel facing straight up. The solar cell output current drops with the Kelly cosine function as shown in Figure 4.2. To minimize power losses due to inclined solar incidence, the MSE design must consider the optimal mounting position and angle of the solar panels. The most optimal flight conditions are at noon in June, with a solar incidence angle of around 46°. However, this still reduces the solar array output by about 30%. If the solar array output should not drop by more than 50%, the maximum solar incidence angle is about 57°. This is only an approximation from the assumption that the solar array is mounted flat on top of the airship envelope, which will not be the exact case in practice.

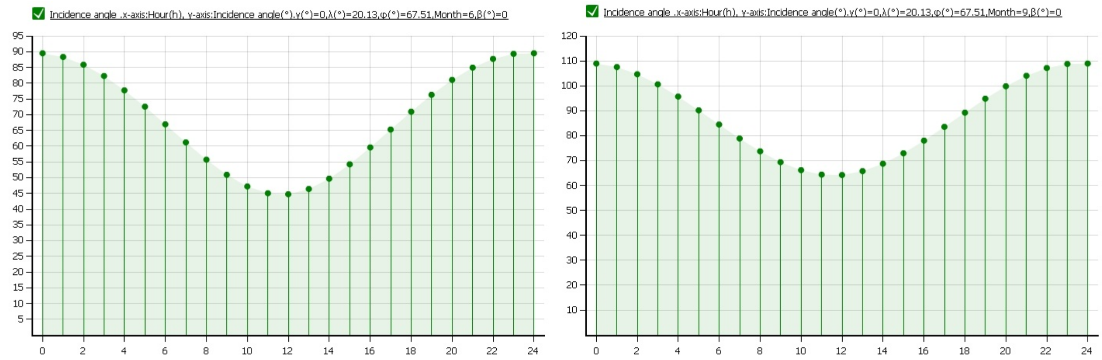

Figure 4.1 – *Monthly average solar incidence angles for June (left) and September (right) for each hour of the day.*

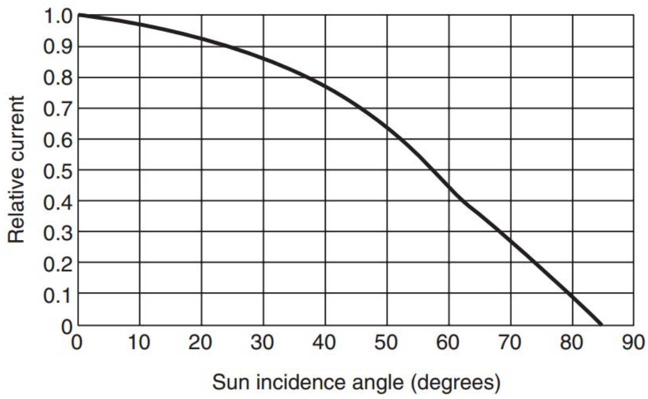

Figure 4.2 – *Kelly cosine function showing how solar cell photo current depends on sun incidence angle onto the solar cell[18, Fig 9.12]*

Solar Array Shading

Shading on the solar panels, for example caused by airship stabilizer structures or objects in the landscape, can cause a significant drop in the cell output voltage, as described in [19, p. 165]. Bypass diodes can be used to partly mitigate this issue. However, since the airship is only expected to fly at altitudes above normal terrain and building height the only shading possibly expected is from the airship structure. Hence the MSE design must consider this restriction.

Battery Temperature

One of the most temperature-critical EPS components is the battery, which must stay within its safety temperature limits. In the proposed design, only temperature monitoring is offered. Therefore, flight is only allowed when outdoor temperatures are well within the allowed battery temperature range. Otherwise a battery heater and more sophisticated thermal design may be necessary.

4.2.4 Expected Performance

The expected EPS performance values are listed in Table 4.4.

Table 4.4 – *Expected performance for the EPS*

Description	Symbol	Value
Power conversion efficiency (SAR)	-	$> 90\%$
Power output (SAR)	P_{out}	$\sim 45\,W$ [a]
Battery capacity	C_{bat}	$7.3\,Wh$
Mass	W_{EPS}	$\sim 980\,g$
Total cost	-	$\sim 12000\,SEK$ [b]

[a] For ideal weather conditions, i.e. no clouds and best expected solar incidence angle

[b] Solar cells are significantly more expensive than anticipated. A request for more funds is under preparation.

4.3 Critical Design

The basic EPS diagram is shown in Figure 4.3. A SAR controls the operating voltage of the solar array and supplies an un-regulated mainbus. The mainbus voltage is mainly controlled by the battery voltage. A DC-DC regulator provides a regulated $5\,V$ supply to subsystems and payloads. The motors are supplied from the unregulated mainbus.

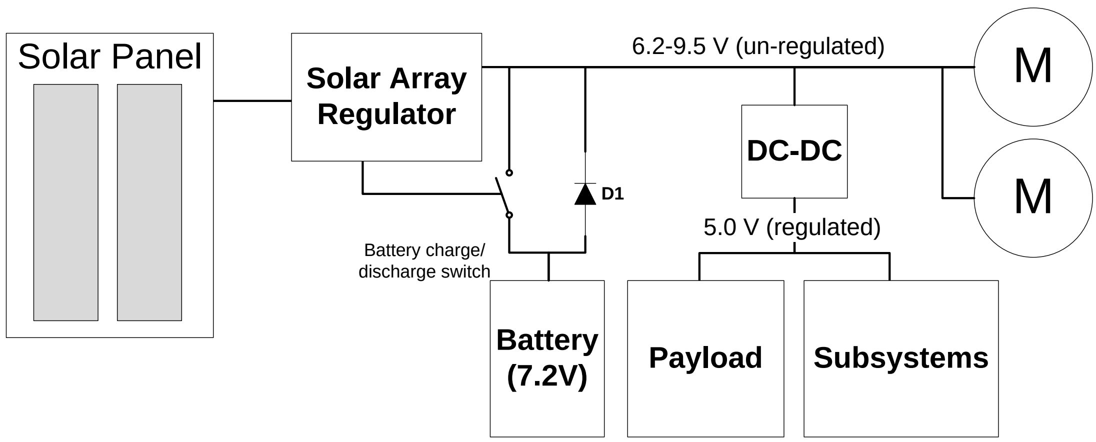

Figure 4.3 – *EPS simple block diagram*

4.3.1 Battery Design

In [15] it was decided that a Li-ion type battery was suitable for the EPS. An *Ansmann Lithium-Polymer (LiPo) Racing Pack 2S1P 30C* battery is selected with the specifications as listed in Table 4.5.

Table 4.5 – *Specifications of selected battery*

Description	Symbol	Value
Chemistry	-	Li-Polymer
Nominal voltage	V_{bat}	$7.4\,V$
Capacity	C_{bat}	$2.1\,Ah$ / $15.54\,Wh$
Weight	W_{bat}	$122\,g$
Dimensions	-	$105\,mm \times 35.2\,mm \times 17\,mm$
Maximum fast charge current	$I_{charge,max}$	$3\,A$
Maximum discharge current (continuous)	$I_{discharge,max}$	$63\,A$

Battery Charge Regulator

The Battery Charge Regulator (BCR) must control the charge rate of the battery such that the charge current limit is not exceeded and it must cut off the charge current when the battery is fully charged. Temperature monitoring is usually also required to inhibit charging if the battery temperature is outside its safety limits.

A *MCP73842* Li-ion battery charge regulator Integrated Circuit (IC) is selected. It employs three different charge modes: low-charge for deeply discharged batteries, Constant Current (CC) charge and trickle charging. It also includes inputs for temperature monitoring. The battery maximum charge current was given in Table 4.5 as $3\,A$. From the *MCP73842* datasheet, the minimum current sense resistor, R_{sense}, is calculated as

$$R_{sense} = \frac{V_{FCS}}{I_{REG}} = \frac{120\,mV}{3\,A} = 40\,m\Omega \tag{4.1}$$

Where V_{FCS} is the fast charge voltage regulation across the sense resistor and I_{REG} is the desired charge current. A $50\,m\Omega$ current sense resistor is selected leading to a charge current of $2.4\,A$. A heat sink must be added according to the thermal calculations in Appendix A.1. In Appendix A.1, heat sink requirements for the BCR transistor are calculated.

Future Improvements

As was calculated above, significant power may be lost in the BCR Metal-Oxide-Semiconductor Field-Effect Transistor (MOSFET). This is due to the selected BCR IC which requires an input voltage of around $9.5\,V$ (including a Schottky diode forward voltage drop and some design margin). In the future, the BCR could be designed to allow operation with an input voltage only slightly above the battery voltage thus minimizing the charge losses and relaxing the thermal requirements of the MOSFET.

Battery Temperature Monitoring

The selected LiPo battery is rated, in charge-mode, for the temperature interval 0 to $+45°C$. For temperature measuring, a $4.7\,k\Omega$ *NTCLE203E3472GB0* thermistor is selected which has a Beta Value, $B = 3977\,K$. Since the battery temperature is measured using an external thermistor, the temperature response is likely to be somewhat slower, so an extra $5°C$ thermal design margin is added. The required resistance values of the BCR temperature control resistors are determined from the *MCP73842* datasheet as

$$\begin{aligned}
R_{cold} &= R_{25}\, e^{B(\frac{1}{T}-\frac{1}{T_0})} = 4.7\,k\Omega\, e^{3977\,K(\frac{1}{278\,K}-\frac{1}{298\,K})} = 12.28\,k\Omega \\
R_{hot} &= 4.7\,k\Omega\, e^{3977\,K(\frac{1}{313\,K}-\frac{1}{298\,K})} = 2.48\,k\Omega \\
R_{T1} &= 2\frac{R_{cold}R_{hot}}{R_{cold}-R_{hot}} = 6.2\,k\Omega \\
R_{T2} &= 2\frac{R_{cold}R_{hot}}{R_{cold}-3R_{hot}} = 12.6\,k\Omega
\end{aligned} \tag{4.2}$$

where R_{25}, R_{cold} and R_{hot} are the thermistor resistance values at room temperature, the low and high temperature limits respectively. R_{T1} and R_{T2} are the required BCR temperature control resistors setting the required temperature interval.

If the sensed battery temperature falls outside the $+5$ to $+40°\,C$ region, battery charging will be inhibited. The technical requirements from Table 4.3 require the EPS to operate down to $-20°\,C$. Hence some insulation and/or heating of the battery may be necessary or flight must be disallowed at outdoor temperatures much below $+5°\,C$.

Battery Under-Voltage Lock-Out

To prevent over-discharge of the battery, a battery Under-Voltage Lock-Out (UVLO) circuit is added as shown in Figure 4.6. An *TL431* precision shunt regulator IC is selected. The lock-out voltage is given as

$$V_{UVLO} = V_{ref}(1+\frac{R_1}{R_2}) = 2.5\,V(1+\frac{29\,k\Omega}{20\,k\Omega}) = 6.125\,V \tag{4.3}$$

where V_{ref} is the *TL431* built-in voltage reference. If the battery voltage drops below this value, the gate voltage to the P-type MOSFET is pulled high, thus opening the switch. The $1\,M\Omega$ resistor adds about $200\,mV$ hysteresis.

The UVLO circuit only cuts out the motor power line. Thus payloads remain supplied and the battery is still slowly drained. This design has been chosen to allow telemetry and telecommand capability during a heavy battery discharge event. In this case, it is expected that all payloads and on-board computers enter a low power consumption mode, to extend the remaining battery supply time. If the battery voltage drops below $5.62\,V$, the $5\,V$ payload power supply shuts down and all telemetry and telecommand capabilities will be lost.

4.3.2 Solar Array Design

The main driver for selecting the solar cell is to choose a part which is very lightweight and easy to mount on the SPA. A *PowerFilm RC7.2-75 (PSA)* solar cell is selected as shown in Figure 4.4. This is a very lightweight flexible solar cell with a PSA backside for mounting. Table 4.6 lists the solar cell specifications.

Table 4.6 – *Specifications of selected solar cell*

Description	**Symbol**	**Value**
Nominal output current	I_{cell}	$100\,mA$
Nominal output voltage	V_{cell}	$7.2\,V$
Nominal output power	P_{cell}	$0.72\,W$
Dimensions	-	$270\,mm \times 90\,mm \times 0.2\,mm$
Weight	W_{cell}	$7.6\,g$
No. of required cells	N_{cells}	100[a]
Total solar array area	A_{array}	$2.43\,m^2$ (assuming $100\,\%$ fill factor)

[a] [20] offers good discount for +100 units order

The solar array is an array of 50 parallel connected strings of two series solar cells as shown in Figure 4.4. The nominal output voltage and current are given as

$$\begin{aligned} V_{array} &= 2 \cdot V_{cell} = 14.4\,V \\ I_{array} &= 50 \cdot I_{cell} = 5\,A \end{aligned} \tag{4.4}$$

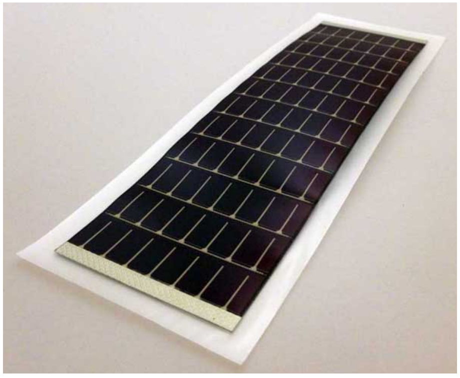

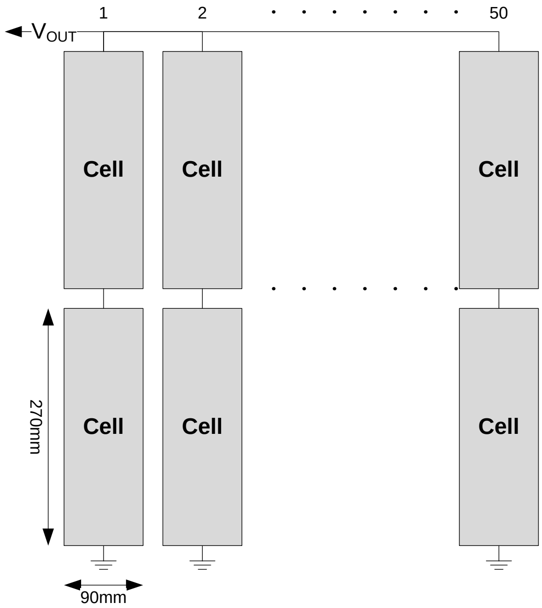

Figure 4.4 – *PowerFilm solar cell (left) and solar array configuration (right)*

Bypass diodes were briefly discussed in section 4.2.3. But since only two cells are connected in series, it is estimated that bypass diodes are not very important in mitigating shading issues since it would require a large amount of diodes (one for every solar cell string) and only one cell is bypassed.

4.3.3 Solar Array Regulator

The SAR must control the optimal solar array operating voltage as well as limit the output mainbus voltage. A simple step-down buck converter topology is preferred for a number of reasons:

- simple circuit analysis and low components count
- no inherent Right Half Plane Zero (RHPZ) in contrary to the standard boost topology
- step-down topology calls for a high input voltage which leads to low input current thus minimizing ohmic losses and the relative forward voltage drop loss from the reverse protection diode

Buck Converter Circuit Design

The ideal transfer function for the buck converter shown in Figure 4.6 is given as

$$V_{out} = D\,V_{in} \tag{4.5}$$

where D is the duty cycle of the MOSFET switch, V_{in} the solar array voltage and V_{out} the mainbus voltage. The duty cycle is controlled by a Pulse Width Modulation (PWM) controller which provides input to a high-side MOSFET driver. A Main Error Amplifier (MEA) measures the mainbus output voltage to generate a control signal for the PWM controller. An *LM3477* chip is selected which combines PWM controller, MEA and gate driver in one IC.

The Current Mode (CM) control scheme is adopted due to its excellent dynamic abilities [21, sec. 12-3-6] and simplified feedback regulator design. A $10\,m\Omega$ precision sense resistor measures the inductor current slope. The *LM3477* has built-in slope compensation to avoid current mode instabilities [21, sec. 12-1].

The converter switching frequency, f_{switch}, is chosen relatively high to $500\,kHz$. The increased switching losses are expected to be outweighed by the fact that the low operating voltage limits switching losses and the high frequency allows the inductor and filter components to be made smaller, thus limiting system mass and the resistive losses in the inductor copper wires which are expected to dominate the converter losses due to the relatively high currents. The inductor current ripple, ΔI_L, can be calculated as

$$\Delta I_L = \frac{V_{in} - V_{out}}{L\, f_{switch}} D \tag{4.6}$$

where L is the inductance and f_{switch} the converter switching frequency. The inductor current ripple is usually limited to about $10\,\%$ of the maximum converter output current leading to a minimum required inductance of

$$L = \frac{V_{in} - V_{out}}{\Delta I_L\, f_{switch}} D = \frac{14.4\,V - 7.4\,V}{10\% \cdot 10.83\,A \cdot 500\,kHz} \cdot 0.514 = 6.7\,uH \tag{4.7}$$

where $10.83\,A$ is the maximum converter output current calculated as

$$I_{SAR,max} = \frac{P_{out,max}}{V_{out,min}} = \frac{65\,W}{6.0\,V} = 10.83\,A \tag{4.8}$$

A $10\,uH$ inductor is chosen giving a current ripple of about $0.72\,A$. If the load current drops below $0.36\,A$, which is unlikely to happen in most operating modes, the converter will enter Discontinuous Conduction Mode (DCM).

For the converter output capacitor, a component is chosen which has very low Equivalent Series Resistor (ESR) and high capacitance to limit the output voltage ripples.

Current Sense Amplifier

With an inductor current ripple of $0.72\,A$ the current sense voltage slope is only

$$v_{sense} = \Delta I_L \cdot R_{sense} = 0.72\,A \cdot 10\,m\Omega = 7.2\,mV \tag{4.9}$$

It is recommended that the slope compensation is equal to or the double of the sense slope [21, sec. 12-1], however the minimum compensation slope is limited to $103\,mV$ by the *LM3477* chip. Thus the sensed slope signal must be amplified, with a gain of around 20 being suitable. This also has the advantage of eliminating some of the typical noise susceptibility in the current sense signal. The current sense circuit in Figure 4.6 consists of two differential OpAmps which amplify the current sense slope. Resistive voltage dividers are placed on the OpAmp inputs to scale down the input voltage signals to always be below the $5\,V$ OpAmp supply voltage.

Since a closed-loop OpAmp gain of 20 is needed at an operating frequency of $500\,kHz$, the gain-bandwidth specification of the OpAmps must be more than $10\,MHz$. The *LTC6362CMS8PBF* OpAmp is selected. One limitation of this OpAmp is its temperature range which only goes down to $0°\,C$. This might be solved by thermally connecting it to the transistor heat sinks or by ensuring that the internal EPS temperature does not go below $0°\,C$.

Input Filter

An input filter is placed in front of the buck converter, mainly to draw a continuous current from the solar array. It also reduces the converters Electromagnetic Compatibility (EMC) issues (see chapter 8). One challenge with the input filter is that it affects the dynamic properties of the converter and if not properly designed, it can degrade the control feedback loop performance. A damping network in the filter is also necessary to avoid instabilities [21, sec. 10-3].

A usable filter has been designed based on PSpice simulations. However thorough analysis still remains to be done to optimize the filter design.

Maximum Power Point Tracking Unit

In [15] it was decided to use a MPPTU with the SAR to increase solar array efficiency during changing environmental conditions. The SAR with Maximum Power Point Tracking (MPPT) can operate in three different operation regions:

- Battery discharge - when the solar array input power is insufficient to cover the load power demand, the battery is slowly discharged in order to maintain the output voltage. The MPPTU controls the input solar array voltage.
- Battery charge - when the solar array input is greater than the load power, excessive power is used to recharge the battery. The MPPTU controls the input solar array voltage.

- Input power limitation - when the battery is fully charged, the regulator will operate the solar array at a non-optimal voltage, thus limiting the input power to keep the output voltage at a maximum limit. The extra potential input power is dissipated as heat externally on the solar arrays.

It is preferred to implement an analog MPPTU mainly since this makes the circuit independent of a control signal from a more complicated external MCU or Digital Signal Processor (DSP), thus allowing a flexible plug'n-play system to be implemented. One challenge with an analog MPPTU is the typical need for expensive analog multipliers [22]. Since the required multiplier only needs to be a first quadrant type (only two positive inputs), it is believed that a low-cost multiplier can be built using standard discrete components [23].

The MPPTU design still remains to be completed.

Mode Transitions

As was discussed in Section 4.3.3, the SAR can operate in three different main modes. The transition between the modes is controlled by the mainbus output voltage as shown in Figure 4.5. If the SAR input power is lower than the load power, the battery will discharge and the mainbus voltage will follow the battery voltage. Once the input power is larger than the load power, the mainbus capacitor will quickly be charged to a voltage higher than the battery voltage. Once the mainbus capacitor voltage crosses the $9.2\,V$ charge threshold, the BCR starts to charge the battery. If the input power is still higher than the combined battery charge power and load power, the mainbus capacitor voltage continues to rise until reaching $9.5\,V$ where the SAR enters the input power limitation mode. The battery may still be charging in this mode. Since the battery is charged with constant current, the input power may be lower than the combined charge and load power but higher than the load power alone. Hence an oscillatory state between battery charge and discharge mode may arise, whose frequency depends on the mainbus capacitance which should therefore be large.

The $9.20\,V$ battery charge threshold voltage is calculated from

$$V_{charge,threshold} = V_{UVLO,BCR} + V_F = 8.90\,V + 0.3\,V = 9.20\,V \tag{4.10}$$

where $V_{UVLO,BCR}$ is the worst-case UVLO threshold voltage of the BCR IC and V_F is the reverse protection diode forward voltage drop.

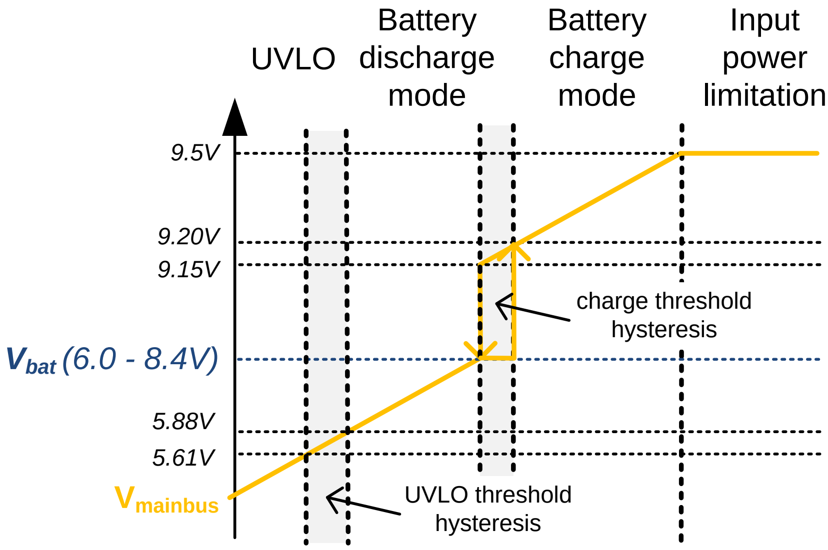

Figure 4.5 – *Different SAR operation modes as function of mainbus voltage*

4.3.4 3.3V and 5V Regulators

To provide regulated 3.3 *V* and 5 *V* supplies for on-board logic circuits and payloads, a *MIC29300-5* Low-dropout (LDO) and a [3.3V regulator name] regulator are selected. Resettable 2 *A* Positive Temperature Coefficient (PTC) fuses are added to protect the loads from excessive currents and to protect the battery in case of a payload short-circuit failure.

4.3.5 Complete Electrical Power System Diagram

The complete EPS diagram is shown in Figure 4.6. Two 17 *A* fuses are added in front of the motors to protect the battery from a motor short-circuit failure.

4.3.6 External Interfaces

The external interfaces of the EPS are listed in Table 4.7.

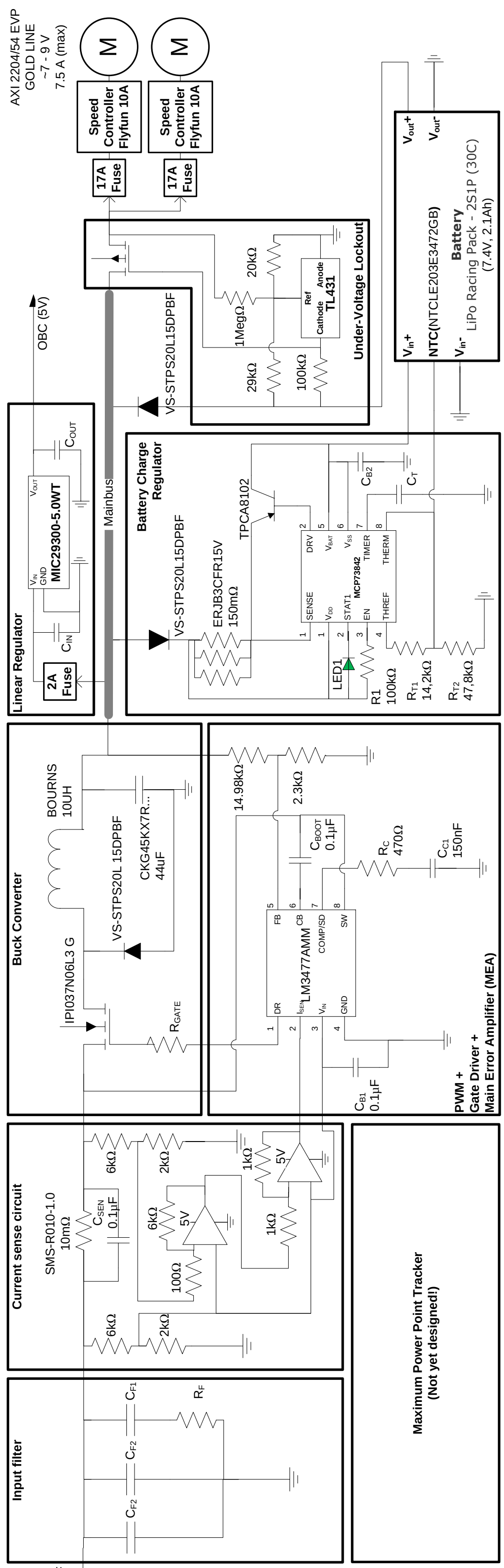

Figure 4.6 – EPS detailed block diagram

Table 4.7 – *EPS external interfaces*

External interface	Type	Implementation
Solar cells mounting	Mechanical	Possibly using PSA - To Be Decided (TBD).
Power electronics mounting	Mechanical	Mounted on a Printed Circuit Board (PCB) which sits in the cargo bay, attached with screws.
Battery mounting	Mechanical	Mounted in cargo bay with strips or Velcro. Thermal insulation with Styrofoam or similar material should be added to protect against cold temperatures.
EPS telemetry	Electrical	Analog signals to microcontroller. Electrical connector interface still remains TBD.
EPS telecommands	Electrical	TBD
Output voltages	Electrical	$6.0 - 9.5\,V$ (un-regulated) and $5.0\,V$(regulated).

4.3.7 Telemetry and Telecommands

The suggested EPS telemetries are listed in Table 4.8 and the suggested telecommands in Table 4.9. Not all telemetries or telecommands are part of the initial EPS design and will only be implemented if time and resources allow it.

The exact electrical configuration and interface connectors still remains to be designed.

Table 4.8 – *EPS telemetry*

Telemetry	Data rate	Data size	Data range
Battery voltage	Every 5 sec	2 bytes	$5\,V$ to $9\,V$
Battery temperature	Every 5 sec	2 bytes	$-25°C$ to $+55°C$
BCR status	Every 5 sec	1 byte	High($5\,V$), low($0\,V$) and $1\,Hz$ 50% duty cycle ripple[a]
UVLO status	Every 5 sec	1 byte	$0\,V$(nominal operation), $5\,V$(under-voltage lock-out)
Mainbus voltage	Every 5 sec	2 bytes	$5\,V$ to $12\,V$
Solar array temperature	Every 5 sec	2 bytes	$-35°C$ to $75°C$
Solar array voltage	Every 1 sec	2 bytes	$10\,V$ to $20\,V$

[a]The different status indications are explained in the BCR IC datasheet

Table 4.9 – *EPS telecommands*

Telecommand	Command signal	Description
Battery charge inhibit	logic low ($< 0.8\,V$) inhibits charging, logic high ($> 1.4\,V$) puts BCR in normal mode	Battery charging can be remotely terminated in case of battery anomalies.
Solar array voltage set	TBD	When MPPT is running, the solar array operating voltage can manually be set to mitigate any malfunction in the MPPT algorithm.

4.4 Test and Verification of Design

This section describes the various design models used to develop the EPS along with the expected functional test to be executed.

4.4.1 Design Models

PSpice Simulations

A transient PSpice simulation model of the whole EPS is currently being implemented. The completed PSpice models are shown in Appendix A.2. These models will help in the design and testing of the regulator performance and system stability during transient loading as well as the interactions between the different circuits.

In the future, it is also desired to implement transient PSpice models for the solar array [24], MPPTU, battery [25], motors and BCR.

Development Model

An EPS Development Model (DM) is currently being built as seen in Figure 4.7. The prototype PCB is realized using self-made "mini-mount" PCB pads as shown in Appendix A.3. These pads are attached, using a simple glue roller, on a complete copper ground plane. This design approach allows a compact layout which reduces parasitic effects. Also any IC package can be supported and parts can easily be moved around when the design changes.

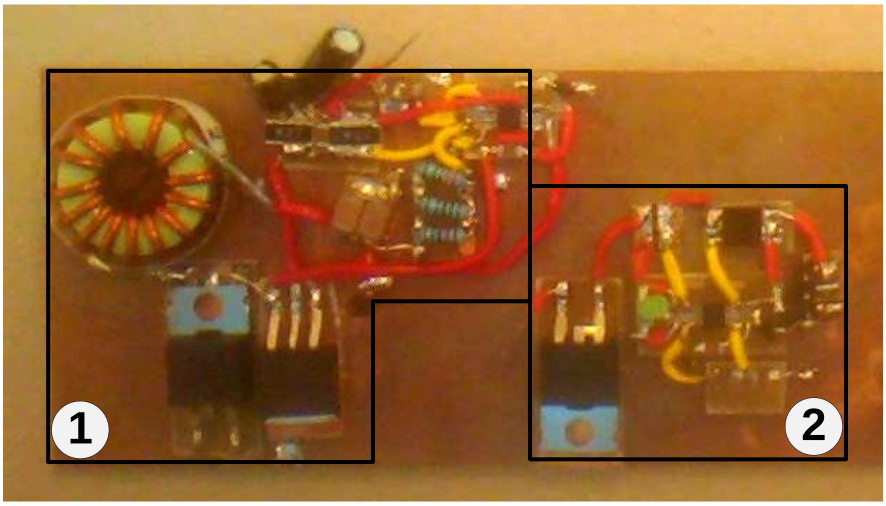

Figure 4.7 – *EPS prototype - **1**: SAR, **2**: BCR*

Development Model Status

The SAR is working but shows signs of CM instability which is probably caused by the missing current sense amplifier circuit and input filter. Development progress is currently awaiting delivery of components. The BCR is also working, however excessive heating of the MOSFET was experienced. A new part rated for higher power dissipation has been selected and is currently awaiting delivery.

Flight Model

If time allows, a dedicated Flight Model (FM) will be built, using a custom designed PCB schematic layout. An optimized PCB layout will minimize the system mass and size while maximizing the efficiency and system robustness.

4.4.2 Test Program

Table 4.10 lists all necessary and desired test of the EPS. Priority "1" tests are all required while priority "2" tests will only be realized if time and resources allow it.

Table 4.10 – *EPS test program*

Subsystem	Condition/Mode	Test Description	Pri.
SAR	Mainbus voltage limitation	With more input power than load power, SAR must be able to maintain a stable 9.5 V output voltage also during transient loading.	1

-	Maximum power handling	With an input and load power slightly above the maximum expected solar array power, no SAR components must overheat or otherwise malfunction.	1
-	MPPT	TBD.	2
-	Mode transitions	SAR must be able to change between MPPT, battery charge and discharge mode without loosing mainbus voltage regulation or causing other malfunctions.	2
-	Feedback loop stability	Regulator bandwidth, gain- and phase margins should be measured with a network analyzer.	2
-	EMC	Electromagnetic emissions should be measured with a spectrum analyzer, especially with regards to the telecommunication systems.	2
BCR	CC and trickle charging	CC charge at $2.4\,A$ and trickle charge mode entered when battery voltage reaches $8.4\,V$ should be verified.	1
-	Charge inhibit at high/low temperatures	While battery is charging, battery thermistor is heated/cooled in thermal oven/fridge to slightly above/below the specified temperature limits and charging should be terminated.	1
UVLO	Power cut-off and recovery	Reducing input voltage below calculated threshold voltage should open switch and switch should close again when input voltage is increased above the threshold.	1
Battery	Dynamic model	Test approach is described in [26].	2
Solar cell	I-V specifications	Short-circuit current, open-circuit voltage, current and voltage at the Maximum Power Point (MPP) should be determined from an irradiance test.	2

-	Temperature coefficients	Solar cell temperature coefficients should be determined by measuring the I-V characteristics at different temperatures within the expected temperature interval.	2
Fuses	Temperature variation	The PTC resettable fuses should be tested at nominal, minimum and maximum expected temperatures to verify acceptable functionality.	1

4.5 Resources

4.5.1 Parts List and Costs

Table 4.11 lists all ordered EPS parts (including one order which is expected to be placed in the near future). The calculated costs do not include invoicing or shipping costs.

Table 4.11 – *EPS Parts list*

Part	Part Name	Supplier	Cost[1]	Qty.
SAR current sense resistor	FCSL110R010FER	Farnell (US)	31.52	2
SAR power diode	MBR3050CT	Farnell	9.24	3
SAR power MOSFET	IPI037N06L3 G	Farnell	19.32	4
SAR mainbus capacitor	CKG45NX5R1C226M	Farnell	38.72	4
PWM, MEA and MOSFET driver	LM3477AMM	Farnell	16.37	5
SAR inductor	2101-H-RC	Farnell (US)	25.13	2
PCBs	CIF - AA15	Farnell	67.42	4
Battery(obsolete)	PA-L60	Farnell	294.28	2
Battery	LiPo Racing Pack 2S1P	Ansmann	N/A[2]	1
Reverse protection diode	VS-STPS20L15DPBF	Farnell	24.56	6
BCR	MCP73842-840I/UN	Farnell	13.61	2
BCR Transistor(obsolete)	TPCA8102(TE12L,Q)	Farnell	28.5	2
Current limit Bipolar Junction Transistor (BJT) (obsolete)	2STN2540	Farnell	7.84	5

Table 4.11 – *EPS Parts list*

Part	Part Name	Supplier	Cost[1]	Qty.
Current limit MOSFET (obsolete)	IRLML6401PBF	Farnell	6.41	2
BCR current sense resistor	ERJB3CFR15V	Farnell	1.97	5
Current limit sense resistor (obsolete)	ERJB2BFR33V	Farnell	4.83	5
Current limit sense resistor 2 (obsolete)	ERJA1BJR27U	Farnell	5.30	5
Power limit BJT (obsolete)	STN888	Farnell	5.49	5
Solar cell	RC7.2-75(PSA)	Eco Power Shop	230.08	2
Solar cell (obsolete)	MC-SP0.8-NF-GCS	Farnell	66.51	2
LDO regulator	MIC29300-5.0WT	Farnell	74.85	2
Current sense OpAmp	LTC6362CMS8#PBF	Farnell	32.31	2
Thermistor	NTCLE203E3472GB0	Farnell	8.64	5
Motor fuses	RGEF1000	Farnell	6.46	5
LDO regulator fuses	MC36248	Farnell	1.41	5
BCR MOSFET	SUP75P03-07-E3	Farnell	31.51	2
UVLO linear shunt regulator	TL431AILPME3	Farnell	1.36	5
UVLO MOSFET	SUP75P03-07-E3	Farnell	31.51	2
Total cost			2707.6	

4.5.2 Electrical Ground Support Equipment

The Electrical Ground Support Equipment (EGSE) in Table 4.12 is mainly required for testing of the EPS.

Table 4.12 – *Required EGSE for EPS*

Instrument	Required Specifications
Network Analyzer	Up to about $\sim 1\,MHz$
Spectrum Analyzer	TBD
Power supply	$75\,W$ output power at $\sim 15\,V$
Heating and cooling chamber(s)	$-20°C$ to $+45°C$ and allow wire interfacing through chamber

4.5.3 Mechanical Ground Support Equipment

The required Mechanical Ground Support Equipment (MGSE) is mainly for PCB manufacturing, i.e. UV light source, photo developing facility, etching facility, drills, cutters etc.

Chapter 5

Motor Control and Communication

The MCC subsystem is responsible for providing sufficient thrust to the airship for its movement and for providing communication with a controller on the ground.

5.1 Functional and Technical Requirements

5.1.1 Functional Requirements

Below are listed the primary functional requirements for the MCC:

- Reliable communication between ground controller (transmitter) and airship (receiver)
- Independent speed control for each of the motors to allow control of flight direction
- Sufficient thrust to propel the airship considering the requirements and flight conditions as discussed in Section 2.2
- Operation of the airship from the ground

5.1.2 Technical Requirements

The technical requirements for the MCC subsystem are presented in Table 5.1.

Table 5.1 – *Technical requirements*

Parameter	**Value**
Total mass	$< 250\,g$
Input voltage	$6 - 9.5\,V$
Average power consumption	$\sim 45\,W$

As it was decided to use a blimp from Esrange instead of the custom-built MSE (see chapter 3), the whole system had to be redesigned. The main changes were the increased dimensions of the blimp and the decreased total lift mass. This required more powerful and efficient motors to cope with the expected increase in wind drag of the SPA. The transmitter/receiver system however remained unchanged.

5.1.3 Expected Performance

The expected performance of the chosen MCC design is listed in Table 5.2.

Table 5.2 – *Expected performance of motors and controls*

Parameter	Value
Total mass	$\sim 55\,g$
Max. current per motor	$7.5\,A$
Max. motor voltage	$11.2\,V$
Number of motors	2
Motor efficiency	$\sim$ 77%
Motor dimensions	$27.6 \times 11mm$
Transmission frequency	$2.4\,GHz$
Receiver channels	6

5.2 Critical Design

The functioning of the MCC subsystem is shown in Figure 5.1. The transceiver consists of a $2.4\,GHz$ transmitter and receiver (see below). The receiver forwards the motor speed control commands to the Electronic Speed Control (ESC) which in turn controls the motor to reach the desired speed.

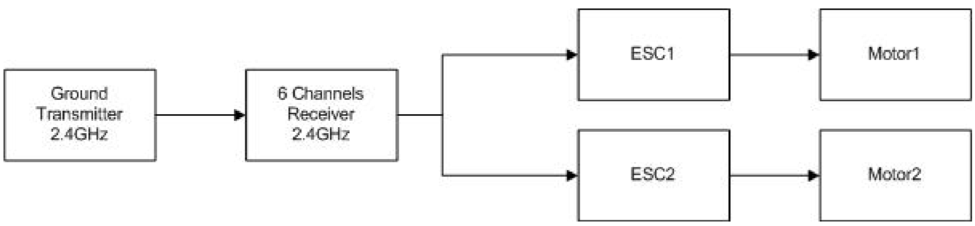

Figure 5.1 – *MCC block diagram*

5.2.1 Motors, Controllers and Propellers

Brush-less motors are selected as they are known to be powerful, durable and light at the same time. Figure 5.2 shows a motor with propeller and connected to an ESC. For the

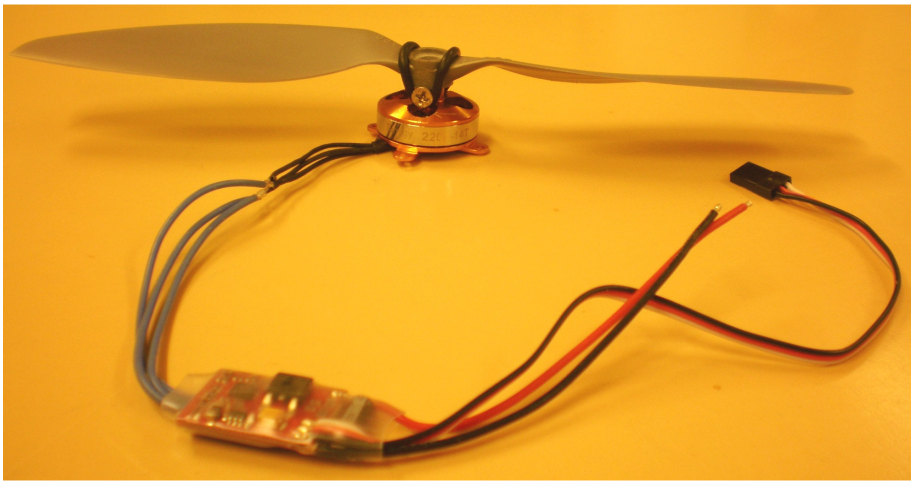

Figure 5.2 – *MCC motor with propeller and ESC*

ECS! (**ECS!**), two alternatives exist:

- Use a Commercial Off-The-Shelf (COTS) ESC for each motor
- Build a motor speed controller using a microprocessor

The primary advantage of using COTS ESCs is the ease of use. This reduces the development cycle to a large extent. The disadvantage of using it is limited scalability i.e. functions like autonomous control and telemetry and telecommanding are not possible. Nevertheless, COTS ESCs will be used to control the speed of the motors because of time constraints. If time permits it will be desirable to build a speed controller with the help of a microprocessor. The new motors however require a higher current than the motors that were originally selected. Therefore suitable ESCs are selected which are able to supply a maximum current of $10\,A$.

5.2.2 Transceiver System

For the transceiver system the available options are to use

- A $72\,MHz$ transceiver system that uses Amplitude/Frequency Modulation
- A $2.4\,GHz$ transceiver system that uses Spread Spectrum Technology

A comparison between these two technologies is shown in Table 5.3. It is clear from Table 5.3 that a $2.4\,GHz$ transceiver system is better for the chosen application. The only disadvantage of using a $2.4\,GHz$ transceiver system is that the receiver should have very reliable batteries and the voltage should constantly be maintained at a particular level since there are small processors in the transmitter and receiver that carry out many complex calculations every second. These processors require a constant steady supply of

Table 5.3 – *Transceiver systems*

Parameter:	$2.4\,GHz$ **Transceiver**	$72\,MHz$ **Transceiver**
Frequency Used	$2.4\,GHz$	$72\,MHz$
Crystal Used	No	Yes
Change in Frequency	On next power up	By changing the crystal
Ability to transmit through obstacles	Weak	Very Good
Bandwidth	Wide	Narrow
Data Rate	High	Low
Power Usage	Low	High
RF Noise Immunity	Very Good	Good

current to work properly. If there is an interruption in the supply current of the receiver there will be problems with the communication channel.

The $2.4\,GHz$ transceiver system is selected for the communication channel. The transceiver uses the $2.4\,GHz$ frequency band and the spread spectrum technology for transmission of signals. This feature helps in removing all interfering frequencies caused by other electronic equipments thus improving the quality of the communication channel. The other major advantage of using spread spectrum technology is that the communication channel is not affected, even when someone is using the same frequency band.

5.3 Test and Verification

Table 5.4 lists completed and scheduled tests of the MCC subsystem.

Table 5.4 – *MCC test program*

Test	Description	Status
Motor control from ground transmitter	Two motors should be controlled from the ground transmitter via the onboard receivers and ESCs.	Completed with success. Some re-programming of ground transmitter is needed to make it more intuitive to use.
Motor thrust measurement	A rack, with the two motors mounted on, is placed on a scale that measures the generated thrust.	Completed, see Figure 5.3. At $\sim 66\,W (\sim 11\,V\ ,\ 6\,A)$ the motors generated a thrust of $\sim 210\,g\,(2.06\,N)$
Communication range	Effective communication range between ground transmitter and onboard receiver should be tested up to at least $250\,m$.	Pending.

Figure 5.3 – *Stationary test of motor thrust level*

5.4 Ressources

Table 5.5 lists the ordered MCC parts.

Table 5.5 – *MCC parts list*

Part	Part name	Supplier
Motor	Turnigy 2204/14 1450 kv (AXI 2204)	www.rcflight.se
ESC	HobbyWing Flyfun 10 A, HW10A	www.rcflight.se
Propeller	APC Slowflyer Pusher 9×4.7	www.rcflight.se
Transmitter	WFly WFT07 2.4 GHz 7-channels	www.rcflight.se

Chapter 6

Imaging and Tracking Payload Unit

The ITPU is the scientific payload of the airship. The purpose of the ITPU is to take aerial images from different positions, acquire accurate position and attitude data and use that combined information to create aerial image maps. This subsystem is in general independent of the airship's control system, but it uses the airship's EPS. It would however be possible in an extended version to also incorporate a controlling interface and to connect the motor ESCs to the computer of the ITPU.

The subsystem is split up into the following parts:

- Attitude determination: use an advanced data fusion method to facilitate GPS, gyroscope, accelerometer and magnetometer information and to extract accurate position and attitude information together with reasonable error estimates.
- Imaging system: provide images with a megapixel resolution webcam in regular timesteps in the order of a second. The image data is saved on a Secure Digital (SD) memory card together with the attitude information for off-line processing.
- Communication system: transmit attitude data and telemetry to a ground station.
- Image processing software: image matching and evaluation on a standard computer after payload recovery.

6.1 Functional and Technical Requirements

The functional requirements of the ITPU are listed below.

- Measure absolute and accurate position and pointing angles
- Take images in regular time-steps and save them together with attitude data
- Receive and execute basic telecommands such as image capture start/stop
- Send basic telemetry data (e.g. position) to a ground station
- Combine single image captures into a large area map

The technical requirements are listed in Table 6.1.

Table 6.1 – *Technical requirements*

Parameter	Value	Remarks
Operation altitude	$< 500\,m^a$	Open air
Input voltage	$5\,V$	Un-regulated
Maximum power consumption	$2.5\,W$	-
Image storage capacity	$>$ 1000	1 Mega-pixel resolution

[a]The U-SPACE requirements are less stringent, but the ITPU might be used at these altitudes in later applications

6.2 Electronic Components

6.2.1 Board Computer

To read out the sensors, communicate with the ground station and save images from the camera, an embedded system which provides all necessary interfaces and sufficient computing power to handle comparably large data streams from the camera is required. The BeagleBone [27, 28] was selected, but only the BeagleBoard [29] was delivered, which is a related predecessor that lacks some features.

The BeagleBoard is a microcontroller board running a TI OMAP3530 ARM Cortex-A8 System on Chip (SoC). It provides 256 MB RAM and several high and low level interfaces. The main interfaces used for the U-SPACE project are Inter-Integrated Circuit (I^2C) and Universal Asynchronous Receiver/Transmitter (UART) for communication with the sensors (gyroscope, magnetometer, accelerometer) and the GPS-receiver and radio-transmitter module (E-TAG). The high level interface to connect the camera is the Universal Serial Bus (USB)-host adapter. The operating system with the control program as well as the image files are stored onto an 8 GB class 10 SD card. The required supply voltage for the BeagleBoard is 5 V. The voltage of the pins on the extension header is 1.8 V.

6.2.2 Sensors

To determine the position and attitude of the airship the LSM303DLM [30] combined magnetometer and accelerometer and the ITG-3200 triple-axis gyroscope [31] from Sparkfun are used. Both sensors have been used by the team members during an earlier project. The sensors communicate via an I^2C interface with the main board at 3.3 V. To receive GPS information an E-TAG device developed by Esrange is used. It is connected via a serial line interface with the main board. It also provides a transmitter module for communication with the ground station which however, will not be used for U-SPACE.

6.2.3 Camera

As high-quality embedded industrial cameras are very highly priced, a consumer webcam with a resolution of several megapixels will be connected to the USB-port of the main board. It is planned to acquire a camera which is supported by the Linux operating system running on the main board.

6.3 Software Environment

The BeagleBoard is equipped with an 8 GB micro-SD card. A Debian-based Linux operating system is installed onto the card providing the environment, libraries and drivers for the program to run. As compared to the BeagleBone the BeagleBoard lacks pull-up resistors on its I^2C interface which produces problems with the Linux kernel. Also, the standard kernel for this board came without the possibility to enable the I^2C controller. Therefore a custom version of the Linux kernel was compiled for the BeagleBoard in order to activate the I^2C device on the extension header.

The OnBoard program is divided into five threads. One thread is responsible for getting the newest sensor data from the accelerometer, magnetometer and gyroscope through the I^2C interface and fusing them to achieve accurate position and attitude representations. This thread is running at a relatively high frequency (>50 Hz, but the final frequency has not yet been defined). A second thread is polling for new GPS data from the E-TAG via a serial line. As the GPS-chip only updates the positional data about once per second this thread can run at a much lower frequency. A third thread is responsible for controlling the camera and if active, it will take a picture every second and save it to the SD-card. The two final threads handle the sending of telemetry data to and the receiving of basic commands from the ground station, respectively.

Due to a lack of time a standard kernel is used which is not hard real-time capable. Nevertheless it still has the possibility of using pre-emptive scheduling which should give a high enough accuracy. It should be noted that in future developments it could be beneficial to use a real-time Linux kernel.

6.4 Image Processing

The provided sensory and computational system (the U-SPACE ITPU) is meant to be a cradle for image processing experiments that simulate low earth orbit conditions. Given the meta-information available from the images, several basic scenarios can be assumed:

- Aerial map creation (optionally automatic)
- 3D reconstruction of large areas
- Object tracking
- Visual attitude determination

The basic design of each possibility and its scientific potential are briefly discussed in this section.

6.4.1 Camera Calibration

A simple and low-cost camera is being used, but, nevertheless, the system has to be calibrated and projection distortion has to be compensated. Since it is assumed that pictures are taken at larger distances than the camera was designed for, this distortion compensation is crucial for a proper output quality. The camera parameters are modelled assuming a simple pin-hole camera. Pictures of a well known pattern with easily detectable lines or points on lines are taken. Taking various pictures of a tilted chess board pattern allows to stably detect corners of the pattern. The corners are lying on a straight line (under a rotation-translation transformation). Using this information the so-called intrinsic camera parameters can be calculated. As the straight lines of points will appear to be curved on the pictures, a transformation can be computed to straighten up these lines and thus compensate for the lens distortion. There might be a need for future extrinsic camera calibration as well. This is important especially for 3D and automated applications where a coordinate frame is required.

6.4.2 Preprocessing

A crucial step for quality assurance is the first preprocessing and data homologization step. The input picture needs to be as clear and dynamically stable as possible as well as distortion free. There might be more steps involved, but the most important ones are lens distortion compensation, contrast and brightness stabilization and blur removal. Lens distortion compensation is a compensation of the lens's radial character and comes as the calibration result. Contrast and brightness might be adjusted globally to avoid saturated or noisy pictures. It is assumed that the aerial carrier is moving and without suitable light conditions the image can get blurry. To compensate for this blur a motion blur removal filter has to be deployed. Assuming linear and constant motion a Wiener filter can be implemented. The motion can be estimated from the sensors or through image analysis.

6.4.3 Aerial Map Creation

Creating an aerial map or stitching partial views into a single picture is a basic space-related operation. The implemented approach consists of the following steps:

1. Preprocessing
2. Feature detection
3. Feature rejection
4. Transformation estimation
5. Transformation
6. Image merging

Preprocessing was described in section 6.4.2. Feature detection is then the next step. As there are many feature detectors there is a possibility to evaluate the performance of different feature detectors on different climates or terrain types. It was decided to implement three feature extraction methods to start with. These methods are the well-known SIFT keypoints, Kanade Lucas Tomasi (KLT) tracker based features and AGAST - a machine-generated corner detector developed at DLR for robust 3D reconstruction.

Feature rejection then filters wrong data or data irrelevant to the transformation that is under investigation. It can also filter bad features, that are not persistent in the pictures long enough. Based on the geometry of the detected features and sensor information affine transformation parameters can be estimated at the minimum. All of these methods should provide enough control points so that it would be possible to estimate an even higher polynomial transformation to ease the image stitching at the edges.

After carrying out the transformation the pictures can be merged with small overlapping regions around the edges, followed by a smooth transition from picture to picture.

This process can be handled by the processing unit on-the-fly such that the ITPU is able to provide a ready-made result.

6.4.4 3D Reconstruction of Large Objects

Another potential application is robust 3D object reconstruction. Having multiple arbitrary views of one large object (for example a castle), it is possible to find regions that are invariant to an affine transformation. With these regions the position and parameters of the camera can be calculated as well as a transformation of the key points. This solution is based on the MSER algorithm and implemented in OpenCV.

6.4.5 Object Tracking

In case the ITPU has control over the steering of the airship a real-time object tracking system could be implemented. Tracking is a modified recognition problem which focuses on real-time performance. A continuous target movement is assumed, which allows to incorporate filtering and movement prediction methods such as a Kalman filter.

6.4.6 Visual Attitude Determination

Another important usage possibility is attitude determination. From the relative transformation in-between images a relative six degrees of freedom pose change can be estimated. Having samples of absolute reference this pose can be cleaned of incremental errors and a long time solution can be tested. Such an algorithm could even be used for planetary and interplanetary localization.

6.5 Attitude Determination System

The Attitude Determination System (ADS) measures and estimates the position and pointing direction of the payload system. This function is crucial for the further use of recorded images, as it provides the reference system and the relative alignment of the recorded images towards each other. In order to produce high-accuracy attitude estimates and to compensate for disadvantages of certain sensor types such as drift and noise, a variety of sensors is used and their data is fused to provide complete attitude information. An overview of the ADS is shown in Figure 6.1.

As can be seen in Figure 6.1, the sensors to be used are:

- GPS receiver: provides absolute position values, but has much high-frequency noise
- Gyroscope: provides accurate relative pointing directions, but experiences drift

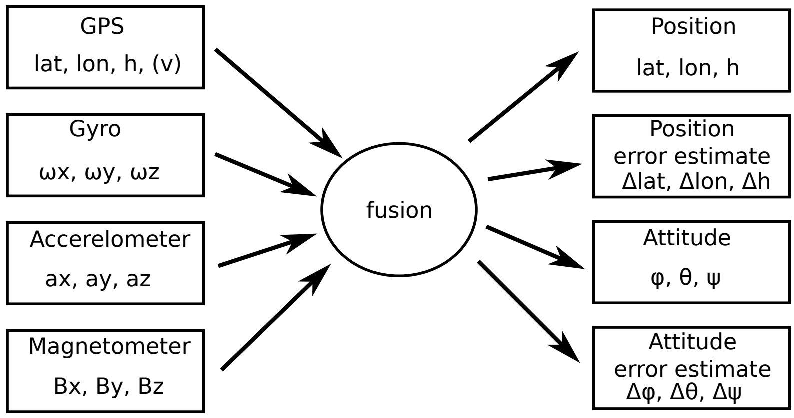

Figure 6.1 – *Attitude Determination System overview*

- Accelerometer: provides absolute pointing relative to the horizon (gravity) and linear acceleration
- Magnetometer: provides absolute pointing relative to the earth's magnetic field

6.5.1 Development Status

The ADS has not only been developed on the final hardware (BeagleBoard). To continue the development during the semester break a recently released Raspberry Pi minicomputer [32] has been privately purchased, with properties very similar to the BeagleBoard. It also runs a derivative of the Debian operating system. A board has been created to attach a complete set of sensors to the system. These sensors are a gyroscope (ITG-3200 from Sparkfun), a magnetometer/accelerometer (LSM303 from Sparkfun) and a GPS receiver(Etag). All sensors are pluggable and the complete system is shown in Figure 6.2(A Venus 6 GPS Module ST22 from SkyTraq has been used in the shown figure). The bottom side of the board including the wiring cables is shown in Figure 6.3. This testing system does not yet contain a camera, but it will be added in the future. In this configuration the entire unit consumes 3 W of power and weighs 71 g (broken down into 30 g for the sensors and shield and 41 g for the computer).

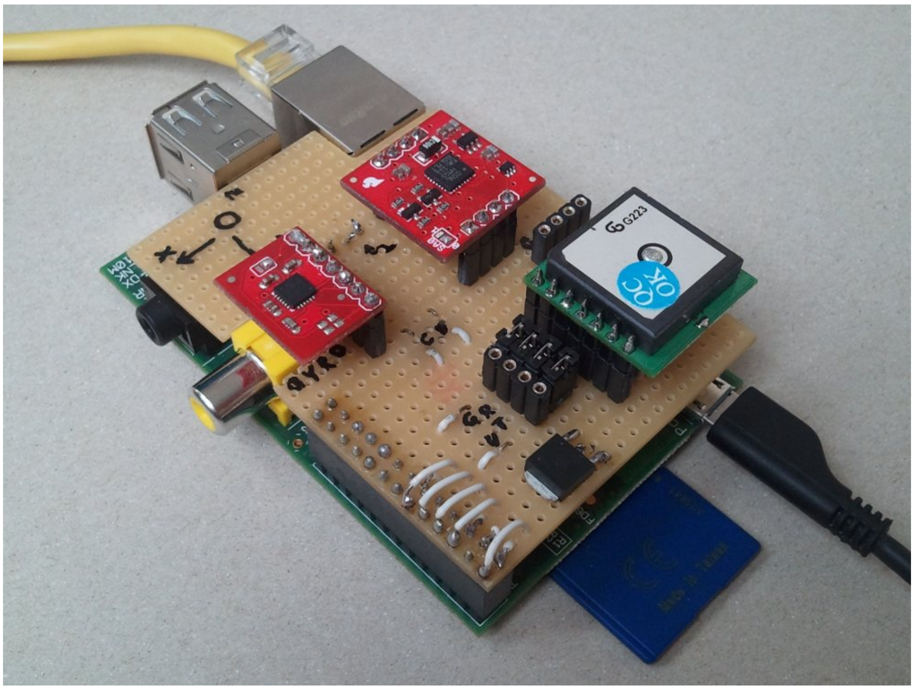

Figure 6.2 – *Top view of Raspberry Pi computer with self-constructed pluggable sensor shield. Mounted on the shield are the gyroscope (red, left), the magnetometer/accelerometer (red, top) and the GPS receiver (green, right). Also I^2C and UART 4-pin sockets are visible as well as a small voltage regulator (bottom) that connects the 3.3 V GPS module to the 5 V high-current source.*

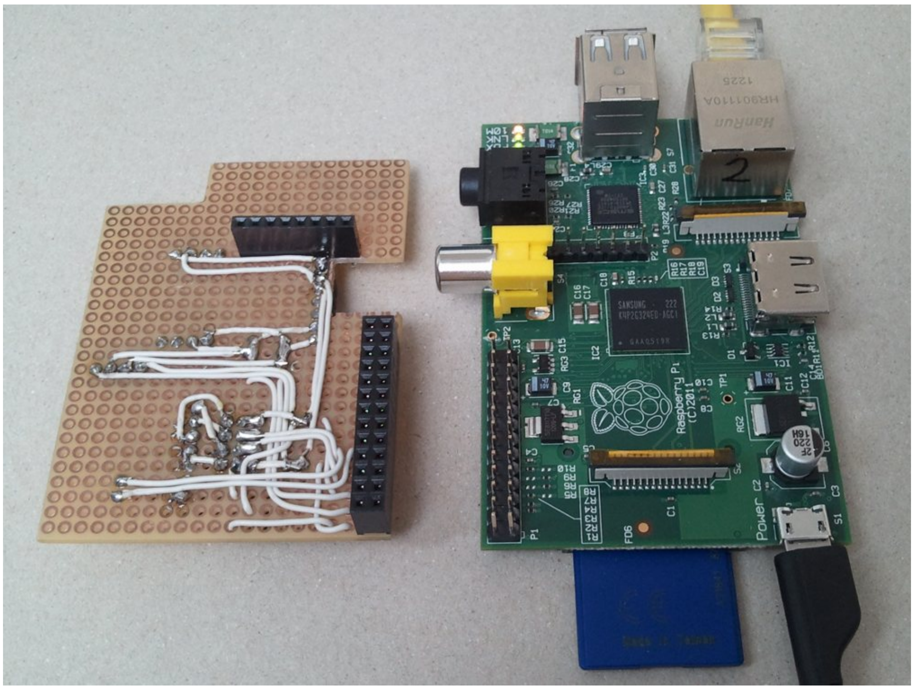

Figure 6.3 – *Bottom view of opened-up Raspberry Pi computer with self-constructed pluggable sensor shield. Wiring from the Raspberry Pi 26-pin P1 header to the individual sensors can be seen on the bottom side of the shield.*

6.5.2 Algorithms

The attitude of the sensing unit could in principle be determined by simply integrating the gyroscope rates from an initial alignment. This measurement however will degrade with time because of significant low-frequency drifts, sensor offsets and measurement inaccuracies. To solve the problem more robustly a combination of 3D gyroscope, a magnetometer and an accelerometer is used. They are fused with a C++ program that runs on the board computer. The main technique used is the Extended Kalman Filter (EKF) which offers a near-optimal attitude estimation with a fixed memory usage. Attitudes are represented as quaternions, which is an elegant and Central Processing Unit (CPU)-effective solution.

Offset filtering for the magnetometer and accelerometer is performed independently. An EKF has been set up that estimates the x- y- and z-offset and the total radius along with each new measurement. The measurements are readily available at system start-up without calibration, but the accuracy will only improve as soon as measurements from different attitudes are available. The EKF also accounts for slow offset drifts and similar effects.

An estimation of the gyroscope offsets and rate scaling is performed with a combination of accelerometer and magnetometer absolute attitude estimations and the gyroscope-integrated attitude. This results in a gyroscope error value at each measurement step that is used by the Kalman algorithm to estimate the system parameters and to calculate a best-estimate attitude.

Finally the position is determined independently from the GPS receiver, which is much simpler than fusing position values from the inertial measurement of the previously described sensors with the absolute GPS position. This approach was chosen due to the tight time constraints of the project. However, in a continuation of the project it is desirable to test the fusion algorithm described in [33, chap. 6.4].

6.6 Electrical Circuits

As compared to the BeagleBone the voltage of the delivered BeagleBoard at the pins of the extension header is only between 0 V and 1.8 V. However, the expected voltage at the supply and at the I^2C interface for the sensors is 3.3 V. Thus additionally to the external pull-up resistors on the I^2C interface also voltage level converters have to be used for the BeagleBoard.

Chapter 7

Thermal Interfaces

7.1 Thermal Requirements

The U-SPACE systems are required to operate in a temperature range of $-20^\circ\,C$ to $+45^\circ\,C$. These limits are based on weather data from Table 2.2 including appropriate design margins. The high temperature limit also considers heat contribution from direct external sun exposure and internal power dissipation from the EPS. Table 7.1 lists temperature-critical parts that are not rated for the full temperature range as given above.

Table 7.1 – *Temperature-critical parts*

Part	**Rating**	**Monitoring**	**Control**	**Protection**
BeagleBoard MCU	$0^\circ\,C$ to $+85^\circ\,C$	-	-	?
EPS Battery	$+5^\circ\,C$ to $+40^\circ\,C$[a]	External thermistor	-	Charge inhibit at low temperature
Current sense OpAmp	$0^\circ\,C$ to $+70^\circ\,C$	-	-	-

[a]Including $5^\circ\,C$ design safety margin

7.2 Thermal Design

From Table 7.1 it is clear that mainly the lower temperature limit is of concern. Currently the U-SPACE thermal design does not include temperature monitoring, except for the battery, nor any temperature control. It will therefore not be possible to fly when the outdoor temperature falls much below $+5^\circ\,C$. This issue may be solved by insulating the cargo bay with Styrofoam or a similar material. Internal dissipation from the EPS and payloads will then increase the internal cargo bay temperature with respect to the outdoor temperature. Additional heaters may also be included in the design, but this will complicate the system and consume power which is already limited.

Complete thermal analysis, insulation requirements and possible heater design still remains to be done.

Chapter 8

Electromagnetic Compatibility

This chapter describes the U-SPACE EMC issues, the Electromagnetic Interference (EMI)-susceptible parts and the mitigation methods. For the U-SPACE EMC one mission-critical circuit has been identified. This is the motor control of the MCC subsystem. Loss of motor control due to EMC issues could in the extreme case result in equipment damage. Two non-critical circuits have been identified as well: the ITPU sensors and the telemetry communication system.

8.1 Electromagnetic Interference Sources

The identified main EMI sources are:

- The EPS SAR: radiated EMI from the power inductor and from high AC-current loops. Also conducted EMI from the power switches
- The two MCC DC-motors: a DC magnetic field (H-field) from the permanent magnet rotor and radiated EMI when the motors are running
- The MCC motor power leads: radiated EMI from large AC-current loops (up to $\sim 7.5\,A$ per motor).

8.2 Electromagnetic Interference Susceptibility

Table 8.1 lists the EMI-sensitive parts which have been identified along with the applied mitigation method.

Table 8.1 – *EMI-susceptible parts and mitigation methods*

Susceptible part	Susceptibility type	Mitigation method
ITPU magnetometer	Constant H-fields	Must be kept at large enough distance from DC-motors. Calibration might be necessary after ITPU integration in complete U-SPACE system.
ITPU sensors	Radiated and conducted EMI	Must be kept at large enough distance from EMI radiation sources.
MCC motor communication	Radiated EMI	Must be kept at large enough distance from EMI radiation sources.
MCC telemetry communication	Radiated EMI	Must be kept at large enough distance from EMI radiation sources.

8.3 Electromagnetic Interference Mitigation Methods

In the U-SPACE project, the primary applied method for reducing EMI-related issues is to separate EMI sources from EMI-susceptible parts by appropriate distances. It is also important to minimize the area of high AC-current loops. This can be achieved by a proper PCB layout of the SAR and by keeping together and twisting the forward and return power leads of the DC-motors. A secondary method of mitigating radiated EMI from the SAR will be to apply shielding either around the complete circuit or only around the power inductor. This will however increase the system mass and is therefore only a last-resort option.

8.4 Electromagnetic Interference Tests

EMI tests for the EPS have been defined in section 4.4.2. In general, susceptibility tests should be applied to the sensible parts defined in Table 8.1. When the EPS SAR and DC-motors are running at full power, no performance/communication degradation or glitches should be noticed due to EMI. Guides for EMI emission measurements and susceptibility tests along with accepted limits are provided in [34].

Chapter 9

Pyrotechnics Interface

In order to achieve the functionality described in chapter 2 there is no need for any form of pyrotechnics. The project does not require the release or deployment of other structures which could make use of pyrotechnics. Therefore pyrotechnics particulars are not discussed in this document.

Chapter 10

Test and Verification of Design

10.1 Design Verification Plan

In order to verify that the goals of the U-SPACE project (as set forth in chapter 2) are truly satisfied after the realization of a prototype, it is very important to perform a series of design verification procedures with this prototype. Verification by analysis, verification by test and verification by inspection are the most important procedures.

10.1.1 Objectives and Responsibilities

A complete design verification plan is an essential element of a successful project. One main objective of having such a plan is the availability of a structure that allows to systematically verify the quality of the work delivered during the project. A design verification plan is also important because it makes it possible to check exactly where problems occur and to find clues towards the solution of these problems.

The responsibility of defining and performing the appropriate design verification procedures for each subsystem lies with the team members responsible for that subsystem. They report to the quality manager and the project manager, who can then define test verification procedures for combinations of subsystems, possibly testing each combination individually. When satisfactory results are achieved the entire prototype can be verified by a final series of procedures.

10.1.2 Verification By Analysis

A first verification method is verification by analysis. This method uses theoretical calculations and simulations to check if the goals of the subsystem and/or project can be realized with the current hardware and software combination [35]. For U-SPACE project these calculations could be a theoretical analysis of the maximum payload mass based on the characteristics of the SPA structure or a comparison of the forces on the structure to calculate the maximum forward velocity due to the motors. Simulations can also be performed for the EPS to check the stability of the provided power or the power consumption of each subsystem (see chapter 4. Comparing the prototype with previously used solution concepts (verification by similarity) can be considered as a subset of this verification method. However, since there are very few examples of a SPA of this type, this specific subset is not used during the project verification phase.

Although calculations and simulations are used extensively during the design phase of the project they are not an essential means to verify the final quality of the subsystem and/or prototype. This type of calculations is very difficult and requires a clear insight in the underlying principles. Since the experience in the team is limited in this respect, the principal verification method is verification by test, which is treated below.

10.1.3 Verification By Test

The second and most important verification method during the U-SPACE project is verification by test. As the name implies this method consists of monitoring the performance and functionality of the subsystem and/or prototype in a simulated test environment [35]. Detailed test procedures and test matrices have to be defined for each subsystem, including such topics as stable basic performance, compliance with other subsystems and extreme conditions. The subsystem or prototype has to achieve satisfactory results in all test procedures to be considered as a successful realization of the project goals.

10.1.4 Verification By Inspection

The final verification method is verification by inspection. It is defined as the visual inspection of hardware and software for good workmanship and compliance to industry or design standards [35]. This method is a very simple method that can give some initial clues regarding the successful design of a subsystem, but which always has to be corroborated by means of test procedures. It is therefore only a minor element in the complete design verification plan.

10.2 Subsystem Test Matrices

The design verification plan of the U-SPACE project includes test matrices for each subsystem, presenting all tests and their (future) results. These matrices can be used to check the progress of the test procedures and are also useful to identify problems with the subsystem. More details regarding the test procedures for each subsystem can be found in the dedicated sections of the specific subsystem chapters.

10.3 U-SPACE Flight Tests

Normally U-SPACE flights require sufficient incident solar power, clear sky, no wind and mild temperatures. However, as of the current writing, the sunlight in Kiruna is disappearing fast and outdoor temperatures are dropping close to zero. U-SPACE will not be ready for flight before late October 2012 (see Section 12.4). Therefore, outdoor flights are not viable this year. Instead it has been planned to execute an indoor test in a large heated hanger at Esrange. This flight allows us to test many important aspects of the U-SPACE system, including:

- Final proof of the Esrange blimp's capability to lift our complete system including payloads.
- Testing our mechanical structure concept and ease of mounting to the blimp.
- Testing of our communication to and control of the motors along with initial aerodynamic properties of a forward propelled blimp and its steering (turning) capabilities.
- Testing of ground station and onboard telemetry and telecommand link.
- Testing of the ITPU payload sensors (attitude and GPS) and camera.

In spring/summer 2013, it will again be possible to perform outdoor flights with U-SPACE thus the primary concept of a solar powered airship can be tested, possibly by the arriving SpaceMasters from round 8. Meanwhile, the power system can easily be tested in laboratory which is already planned (see Section 4.4).

Chapter 11

Ground Support Equipment

11.1 Electrical Ground Support Equipment (EGSE)

The design, construction and test of a SPA requires the use of extensive EGSE, especially during test flights. The EGSE can be divided into the ground station, the controller and some supplementary material.

11.1.1 Concept

The ground station of the U-SPACE project is responsible for receiving data from the scientific payload and combining this data with images taken by the camera. This combination is then used to form aerial maps of the environment (see chapter 6). It can also be used to track the airship with the help of the GPS module and to visualize all data received from the airborne vehicle.

The controller is used to control the SPA during flight (tests). It consists of a basic commercial transmitter/receiver that allows a human ground-based pilot to remotely control the motors of the airship. More information can be found in chapter 5.

The supplementary material of the EGSE consists of a single power supply to charge the battery before flight. This allows the airship to start flying even without the presence of sunlight.

11.1.2 Hardware Description

For the ground station, the hardware is a desktop computer or laptop connected to a receiver. The basics of this system are described in chapter 6. The pictures taken by the camera can be downloaded after flight (requiring a connection between the camera and the computer) or can be sent to the ground station when the SPA is still airborne (via the same wireless connection used by the scientific payload data). The user is presented with visualizations of the scientific data as well as aerial maps constructed from the camera images and the scientific data (see chapter 6 for more information).

The hardware of the controller is basically a commercial remote controller capable of transmitting and receiving. By adjusting the controls the pilot is able to give more or less power to the motors mounted onto the airship. This is the principal means of forward propulsion. This controller system is described in more detail in chapter 5.

Finally, the supplementary material consists of a commercial power supply that is able to charge the batteries of the EPS. The characteristics of this battery are discussed in chapter 4.

11.1.3 Software Description

The supplementary power supply and the controller do not require any additional software. Only for the ground station additional software has to be developed, capable of reading the scientific payload data (received via the wireless connection) and visualizing this data for the user. In order to combine the aerial camera images and the scientific data a custom algorithm has to be written. This software is further described in chapter 6.

11.1.4 Compliance

Both the ground station receiver and the controller transmitter/receiver have to comply with the Radio Regulations of the ITU [13]. As both hardware devices are commercial, no problems are expected in this respect.

11.2 Mechanical Ground Support Equipment (MGSE)

Apart from the EGSE, also a certain amount of MGSE is required for the success of the U-SPACE project. First of all facilities at LTU Rymdcampus, IRF or Esrange have to be available during flight tests to enable on-site fuelling of the envelope with a suitable gas (see chapter 3 for more details). These facilities include a large gas tank, valves and tubes to connect the tank to the envelope and also safety equipment to ensure that the entire procedure does not harm the persons involved.

Secondly an extensive safety system is necessary to prevent the airship from flying beyond the flight test perimeter in case of failures or unexpected weather conditions. This system should nevertheless allow the SPA to move freely during all flight test procedures, without interfering with the normal operation of the airship. Possible implementations include a long rope tied to a fixed point or a cable firmly anchored to a movable object.

Chapter 12

Project Management

12.1 Organisation and Responsibilities

A project of the extent of U-SPACE, even though it is a student project, requires clear agreements between the team members with respect to responsibilities, work load and communication. Also the available support facilities and other practical issues have to be investigated beforehand.

12.1.1 Key Personnel and Responsibilities

Two important team members in the U-SPACE project are the quality manager and the project manager. These managers have been elected by the entire team. The quality manager, Morten Olsen, takes care of the technical side of the project. He is responsible for topics such as technical consistency between the different subsystems, follow-up of the progress of each subsystem and finally for guaranteeing the general technical quality of the project. The quality manager therefore gathers updated information from each subsystem, synthesizes this information and informs the project manager when problems arise.

The project manager, Dries Agten, has responsibilities ranging from practical organisation over general communication to project documentation. The practical organisation includes organizing a weekly meeting, checking meeting reports, etc. With regards to communication the project manager is responsible both for internal and external communication. Therefore the project manager is in direct contact with the supervisors, Kjell Lundin and Alf Wikström. The progress of the project is communicated and regular meetings are held to discuss this progress. The internal communication topics range from calls for meetings to the passing-on of important information gained from the contact with the supervisors. Taking care of the project documentation finally means that the project manager is responsible for the design reviews, the meeting reports and other documentation that may be generated over the course of the project. Currently Morten Olsen has taken over the responsibilities of Dries Agten as the project manager of the U-SPACE project.

Update on Project Structure and Resources

Due to some administrative issues, work on U-SPACE was heavily limited during the spring semester. As a result, a large amount of work remains to be done in the fall semester in Kiruna. Since only four students will actively work on U-SPACE during this semester, it has been decided to extended the amount of course credits for each student from 7.5 ECTS to 15 ECTS. The four students are: Pedro Cervantes, Jan Sommer, Omair Sarwar and Morten Olsen. From fall 2012, Thomas Kuhn will also take over the supervising responsibilities of Alf Wikström.

12.1.2 Functional Organigram

A functional organigram presenting the different subsystems (as defined in chapter 1) and the associated team members is shown in Figure 12.1. This organigram is based on the background and expertise of the different team members (see Table 12.1), such that each team member is assigned a responsibility which he is able to handle.

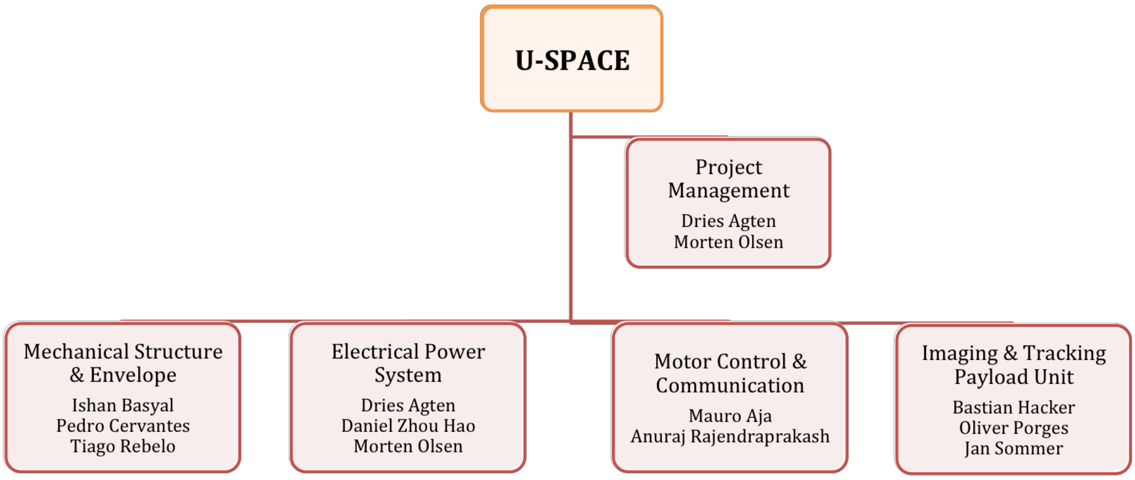

Figure 12.1 – *Functional organigram*

12.1.3 Support Facilities

U-SPACE is mainly supported by LTU through practical, financial and technical support for the team members. The practical support consists of providing tools and specific work spaces, such as mechanical workshops or electronics laboratories. Other aspects are discussed in more detail in section 12.2.

U-SPACE also receives support from Esrange and IRF. Esrange provide launch infrastructure, helium gas and have agreed to borrow us a blimp for testing of U-SPACE. IRF

Table 12.1 – *Background of team members*

Name	Background
Dries Agten	M.Sc. Eng. - Nanoscience & Nanotechnology
Mauro Aja	B.Sc. Eng. - Electronic and Computer Engineering
Ishan Basyal	B.Sc. Earth and Space Sciences
Pedro Cervantes	B.Sc. Eng. - Aeronautical Engineering
Bastian Hacker	B.Sc. Physics
Daniel Zhou Hao	B.Sc. Eng. - Aerospace Engineering
Morten Olsen	B.Sc. Eng. - Electrical Engineering
Oliver Porges	B.Sc. Cybernetics and Measurement
Anuraj Rajendraprakash	B.Tech. Electronics Engineering
Tiago Rebelo	B.Sc. Eng. - Aeronautical Engineering
Jan Sommer	B.Sc. Computational Science

mainly helps as technical consultants in different technical fields and they also provide some parts and has allowed us to borrow some test equipments.

12.1.4 Transport

The transportation of the prototype SPA is an important topic in this project. Since the prototype will be built at the Rymdcampus of LTU and the test flight will most probably take place at Esrange (about 30 km apart), a secure transport procedure has to be developed. As the envelope (blimp) is the property of Esrange (see chapter 3), the complete assembly of the airship will only take place at this location, which relaxes the transport constraints somewhat. Most subsystems are limited in size and can easily be transported in a normal passenger car. The only exception is the solar array and its supporting mechanical structure which might be difficult to fit inside a car. A closed trailer or small truck might be needed for the transportation of this component.

12.2 Relation With Support Facilities

The support facilities mentioned in the previous section play an important role in the course of the U-SPACE project. Their responsibilities are wide, ranging from reports over components to finances.

12.2.1 Reporting and Monitoring

During the entire project the team is monitored by the supervisors Kjell Lundin (IRF) and Alf Wikström (LTU). This monitoring task consists of controlling the budget, approving the ordering of components and evaluating the (technical) progress of the team at strategical points in time. Weekly meetings between the two supervisors and the two team managers are scheduled to identify, discuss and solve all issues that have come up since the last meeting. Apart from these weekly meetings, communication via email and telephone is used to keep the supervisors updated about the status of the project and to ask for assistance when needed.

12.2.2 Reviews

Three main reviews are planned for the U-SPACE project:

- Preliminary Design Review
- Critical Design Review
- Flight Readiness Review

The first two reviews are also the points in time when grades are connected to the work executed up to those points. Each review is briefly described below.

Preliminary Design Review

The PDR was held and approved in early April 2012. With the help of five separate documents, the general project and the four different subsystems were introduced to the supervisors, with a focus on the preliminary design concepts. The supervisors' approval of the PDR made the project budget available and allowed the ordering of the first components.

Critical Design Review

In the Critical Design Review (CDR), which is the current document, the final designs of the subsystems are presented, together with some early verification and prototype results. An oral team presentation was held already in the middle of June 2012, since many team members had to leave the city of Kiruna. The goal of the CDR is to ensure that the complete system design will meet the functional requirements from chapter 2 together with the technical requirements stated for each subsystem in their respective chapters. It must also show that all system interfaces between the different subsystems or the environment are compatible.

Flight Readiness Review

A third optional Flight Readiness Review (FRR) is also planned (see section 12.4). This review is to be held prior to flight, to ensure that all systems are fully functional and compatible with each other and to check that all support equipment needed for a successful flight is available. This review is important since flight events at Esrange are expensive and the availability of the Esrange facilities and help from the staff is limited.

12.2.3 Component Ordering

The ordering of the components is the responsibility of LTU, the university that is also responsible for the project financing (see section 12.3). The members of the subsystems select the appropriate components and pass the order on to the project manager. He consults with the project supervisors and after approval the components are ordered, usually by Lars Jakobsson (LTU). Components are preferably ordered from inside Sweden, but international orders have also been possible.

12.3 Financing

The U-SPACE project is financed by LTU, the principal support facility. For each European team member, the team receives 2,000 SEK, amounting for a total budget of 14,000 SEK. This budget has to be used for the ordering of all components and for any other expenses that might arise during the course of the project (e.g. tools, processing, etc.). An increase in the budget can be realized after an application procedure and approval by LTU. As of this writing, the U-SPACE project still has 4,824 SEK left of its initial budget. As was mentioned in Table 4.4, a request for more funds for the EPS is under preparation.

12.4 Schedule and Milestones

Since the U-SPACE project is a student project that has to be realized within a limited amount of time a tight schedule and a clear definition of important milestones are vital for the success of the project. The schedule has to be updated regularly to reflect the current progress and/or delays of the project. The most recent schedule is shown in Figure 12.2. All important milestones and test programs are indicated as well.

12.5 Configuration Control

Although the U-SPACE project is limited in size, configuration control remains an important element of the success of the project. With four different subsystems and many different team members it is essential to have a common platform where design changes can be listed, tracked and discussed. This is necessary to guarantee technical consistency and to avoid misunderstandings that may endanger the outcome of the project.

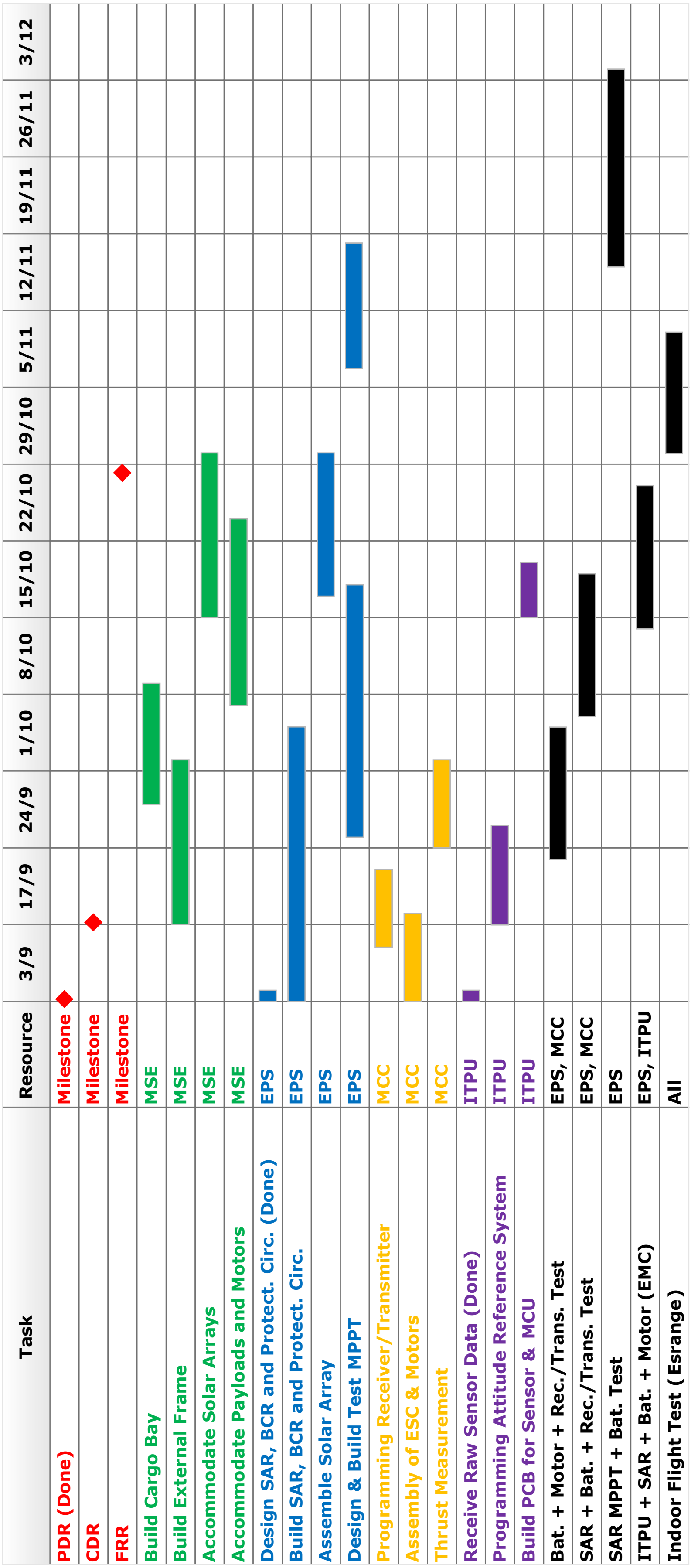

Figure 12.2 – *Project schedule*

The main component of the U-SPACE configuration control is a weekly meeting of all team members. An agenda is composed beforehand by the meeting chair, listing all important issues, both practical and technical, that have to be discussed during the meeting. A meeting secretary is responsible for the minutes of the meeting. These minutes, together with the agendas, are accessible for the entire team via Google Docs. Another component of the configuration control is the revision control system GitHub, which is mainly used to share the documents that make up the design reviews. It is also the place where the developed ITPU code is made available to the relevant team members. For minor issues, emails to a common team email address are used.

12.6 Deliverables

The ultimate goal of the U-SPACE project is to realize a functioning prototype of a SPA capable of forward propulsion while supporting a scientific payload. Since this project is a student project under the supervision of LTU, the final phases of the project also require the handing in of several deliverables.

12.6.1 Hardware and Software

The main deliverable is a functioning prototype of a SPA, consisting of several separately developed subsystems (see chapters 3 through 6). Each subsystem should function on its own as well as in concurrence with the other subsystems. All necessary components have to be included when the subsystem is delivered.

Also the ground station is a deliverable, although it is mainly software-based. All code has to be delivered at the end of the project, together with comments that explain the code (see the following subsection). Also the code written for the airborne part of the ITPU has to be included.

12.6.2 Documentation

The deliverable documentation first of all consists of the two major design reviews (PDR and CDR), which are documents that provide details on the functioning of each subsystem and on the general elements of the project (see subsection 12.2.2). When available, all documents that were used during the development of a subsystem should be classified and stored for future use. This allows future team members to easily pick up the work where it was left by their predecessors.

Apart from these hardware-related documents, documentation regarding the developed software should also be delivered. This documentation mainly consists of comments in the code such that it may be understood and developed further by future team members.

Bibliography

[1] Raven Aerostar. *High Altitude Airships*. http://ravenaerostar.com/products/aerospace/high-altitude-airships. [Online: accessed 15th March 2012].

[2] Nortávia. *Mission*. http://www.id-nortavia.com/gaya/Mission.html. [Online: accessed 15th March 2012].

[3] Julia Saba et al. *Science Enabled By A High Altitude Airship (HAA)*. http://sec.gsfc.nasa.gov/th_poster_HAA.pdf. [Online: accessed 17th March 2012].

[4] Anthony Colozza. *Airships for Planetary Exploration*. Tech. rep. Analex Corporation, 2004.

[5] Projet Sol'R. *Projet Sol'R*. http://www.projetsolr.com/english/. [Online: accessed 11th June 2012].

[6] Russel Woolard. *12 Miles High: An Integrated Airship-Radar Is on the Horizon*. http://www.mitre.org/news/digest/defense_intelligence/03_10/isis.html. [Online: accessed 20th August 2012]. 2010.

[7] Helios Airships. *Helios Airships*. http://www.solarairship.net/index.php. [Online: accessed 15th August 2012].

[8] Solar Ship Inc. *Solar Ship*. http://solarship.com. [Online: accessed 30th June 2012].

[9] M. Thomsen and R. Kirt. *Project Knarr*. http://projectknarr.wordpress.com/. [Online: accessed 29th August 2012].

[10] M. Lundin and U. Svensson. *Luftskeppens Återkomst - Rapport 2*. http://www.energimyndigheten.se/Global/Om%20oss/Vindkraft/Andra%20forskningsprojekt/Luftskeppens%20%C3%A5terkomst%20-%20rapport%202.pdf. [Online: accessed 29th August 2012].

[11] R. Kirt and M. B. Thomsen. *Patent: Wind Turbine Generator Installation by Airship*. http://www.faqs.org/patents/app/20120091274. [Online: accessed 29th August 2012].

[12] Weatherspark. *Average Weather For Kiruna, Sweden For May*. http://weatherspark.com/averages/28941/5/Kiruna-Norrbotten-Sweden. [Online: accessed 20th March 2012].

[13] Panel on Frequency Allocations and Spectrum Protection for Scientific Uses; Committee on Radio Frequencies; National Research Council. *Handbook of Frequency Allocations and Spectrum Protection for Scientific Uses*. The National Academies Press, 2007.

[14] Swedish Transport Agency. *The Swedish Transport Agency's regulations on unmanned aircraft systems (UAS)*. 2009.

[15] M. Olsen, D. Agten, and Z. Hao. *Preliminary Design Report - Electrical Power System*. Tech. rep. USPACE-PDR-EPS-A1. Luleå University of Technology, 2012.

[16] Aerostar International. *TIF-250/460*. http://ravenaerostar.com/products/aerostats/tif-250-460. [Online: accessed 4th September 2012].

[17] Asset Management Consulting Corporation. *SaECaNet - Calculation of Incidence angle to Photovoltaic array and Solar altitude*. http://www.saecanet.com/calculation_page/000433_000562_incidence_angle.php. [Online: accessed 1st September 2012].

[18] R. P. Mukund. *Wind and Solar Power Systems - Design Analysis and Operation*. Second Edition. CRC Press, 2006.

[19] Mukund R. Patel. *Spacecraft Power Systems*. CRC Press, 2005.

[20] Avnet Express. *RC7.2-75 PSA*. http://avnetexpress.avnet.com. [Online: accessed 12th June 2012].

[21] R. W. Erickson and D. Maksimovic. *Fundamentals of Power Electronics*. 2nd edition. Kluwer Academic Publishers, 2001.

[22] Z. Liang, R. Guo, and A. Huang. "A New Cost-Effective Analog Maximum Power Point Tracker for PV Systems". In: *IEEE* (2010).

[23] K. R. Radhakrishna. *Lecture 19 - Analog Multipliers*. http://www.youtube.com/watch?v=_xGqfXiUkqk&feature=related. [Online: accessed 22nd August 2012].

[24] L. Castañer and S. Silvestre. *Modelling Photovoltaic Systems using PSpice*. John Wiley & Sons, 2002.

[25] S. Gold. "A PSPICE Macromodel for Lithium-Ion Batteries". In: *IEEE* (1997).

[26] M. Chen and A. R. Gabriel. "Accurate Electrical Battery Model Capable of Predicting Runtime and I-V Performance". In: *IEEE Transactions on Energy Conversion* (2006).

[27] Beagleboard.org. *BeagleBone*. `http://beagleboard.org/bone`. [Online: accessed 28th April 2012].

[28] Gerald Coley. *BeagleBone System Reference Manual*. 2012.

[29] Beagleboard.org. *BeagleBoard-xM Product Details*. `http://beagleboard.org/hardware-xM`. [Online: accessed 10th May 2012].

[30] *LSM303 Data Sheet*. SparkFun Electronics. Colorado, USA.

[31] *ITG-3200 Data Sheet*. SparkFun Electronics. Colorado, USA.

[32] Raspberry Pi Foundation. *Raspberry Pi*. `http://www.raspberrypi.org`. [Online: accessed 15th May 2012].

[33] P. S. Maybeck. *Stochastic Models, Estimation and Control*. Academic Press, 1982.

[34] *Space engineering - Electromagnetic compatibility*. ECSS-E-ST-20-07C. European Cooperation for Space Standardization.

[35] *Space engineering - Verification*. ECSS-ST-10-02C. European Cooperation for Space Standardization. 2009.

Appendix A

EPS

A.1 Components Thermal Calculations

Battery Charge Transistor

The worst-case power dissipation in the BCR transistor happens when the battery is charged from its minimum charge state

$$\begin{aligned} P_{transistor,max} =& (V_{in,max} - V_F - V_{bat,min}) \cdot I_{charge} \\ =& (9.5\,V - 0.3\,V - 5.5\,V) \cdot 2.4\,A = 8.88\,W \end{aligned} \tag{A.1}$$

where $V_{in,max}$ is the maximum mainbus voltage, V_F the expected Schottky diode forward voltage drop and $V_{bat,min}$ is the preconditioning threshold voltage of the BCR IC. A *SUP75P03-07-E3* P-channel MOSFET is selected for the BCR charge transistor which has a maximum allowed heat dissipation of

$$P_{MOSFET,max} = \frac{T_J - T_A}{\theta_{JA}} = \frac{175\,°C - 45\,°C}{62.5\,°C/W} = 2.08\,W \tag{A.2}$$

Thus requiring a heat sink of

$$\begin{aligned} \theta_{SA} &= \frac{T_J - T_A}{P_{D,max}} - \theta_{JC} - \theta_{CS} \\ &= \frac{175°C - 45°C}{8.88\,W} - 0.8°C/W - 0.2°C/W = 13.64°C/W \end{aligned} \tag{A.3}$$

Battery Charge Diode

A *STPS20L15DPBF* Schottky diode is selected with maximum allowed heat dissipation

$$P_{diode,max} = \frac{T_J - T_A}{\theta_{JA}} = \frac{125\,°C - 45\,°C}{40\,°C/W} = 2\,W \tag{A.4}$$

Heat dissipation in diode

$$I_{carge} V_F = 2.4\,A \cdot 0.3\,V = 0.72\,W \tag{A.5}$$

No heat sink is required for the diode.

A.2 PSpice Simulations

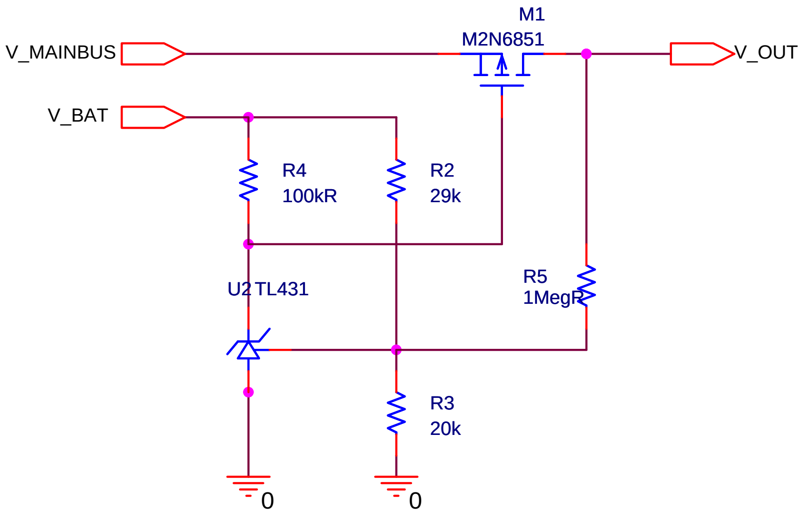

Figure A.1 – *EPS UVLO circuit (PSpice)*

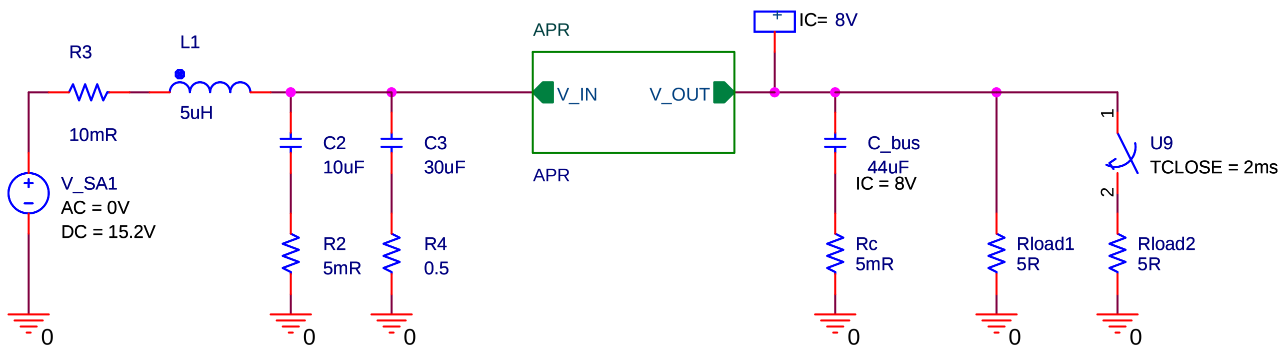

Figure A.2 – *EPS mainbus (PSpice)*

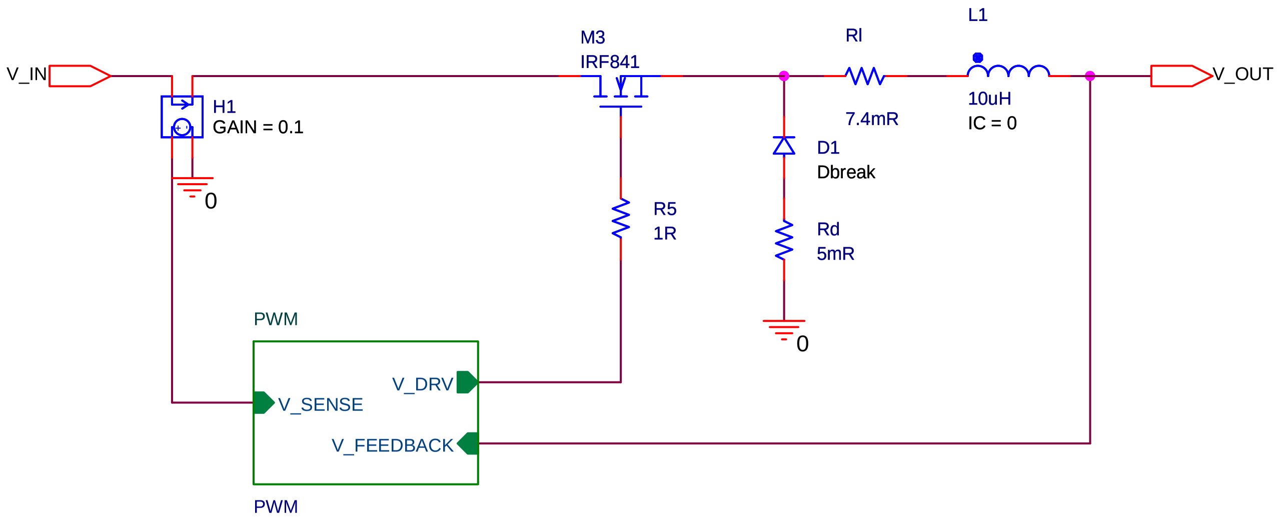

Figure A.3 – *EPS SAR (PSpice)*

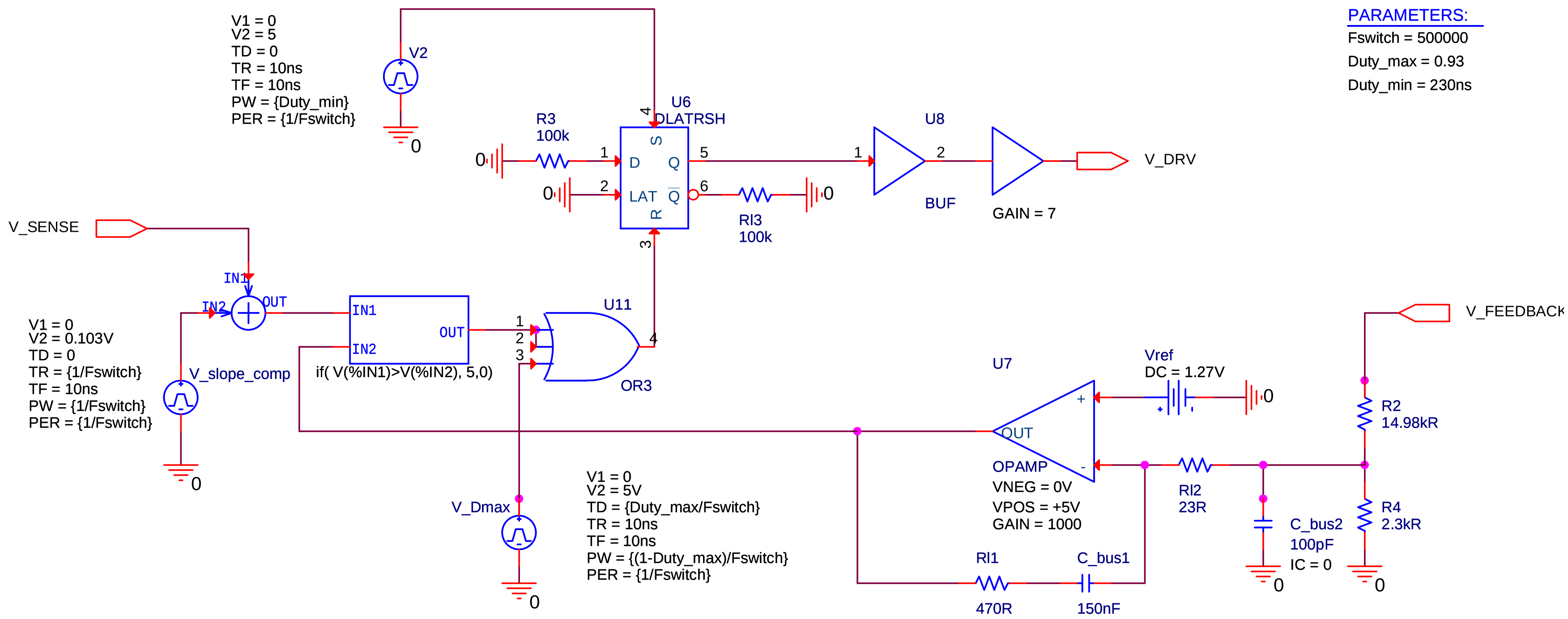

Figure A.4 – *EPS PWM controller (PSpice)*

A.3 Mini-Mount Image

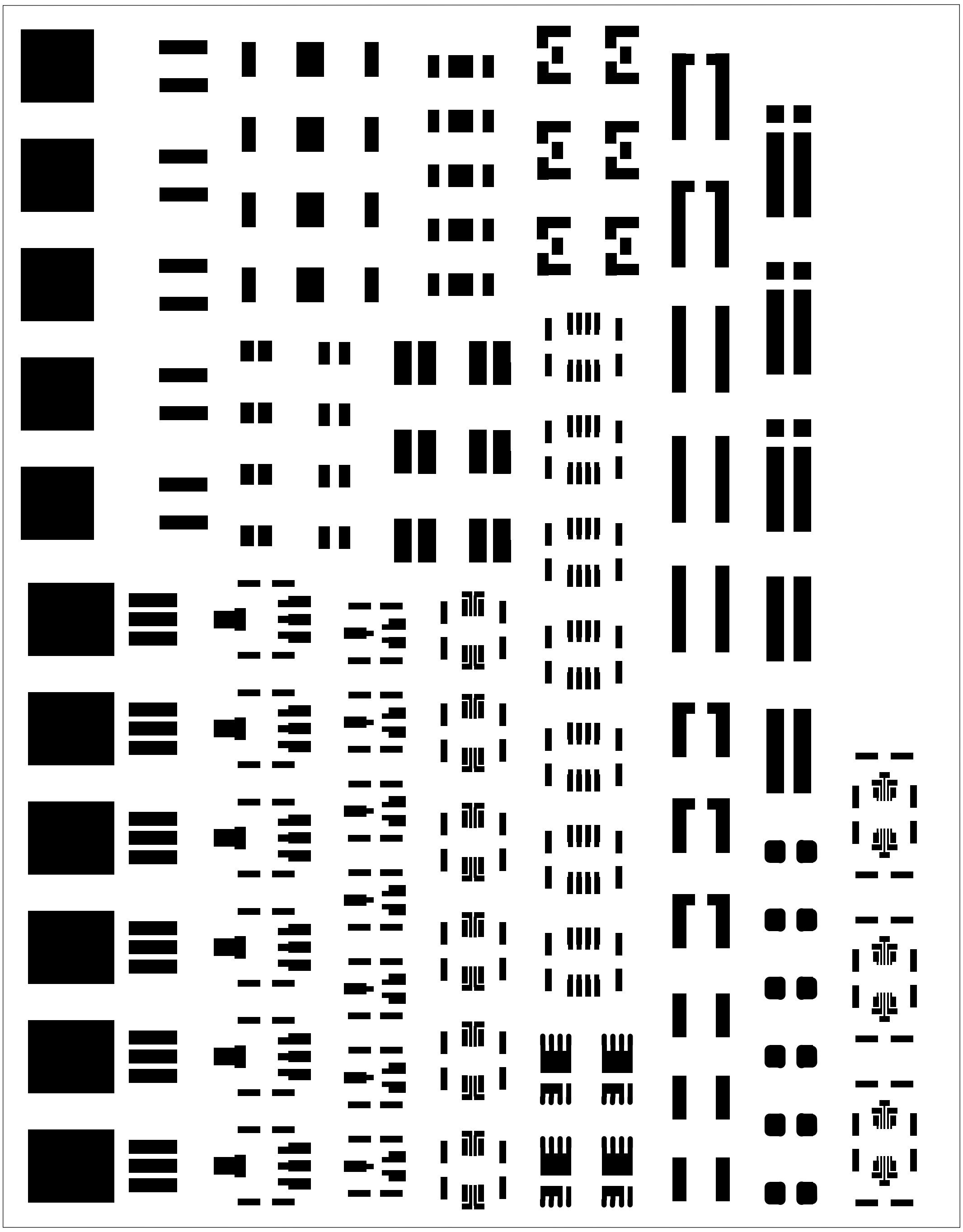

Figure A.5 – *Mini-mount prototype patches*